15100

THE TIME-DEPENDENCE OF THE LOCAL STELLAR VELOCITY DISTRIBUTION

by

JOHN BYL

B.Sc., University of British Columbia, 1969

A THESIS SUBMITTED IN PARTIAL FULFILMENT OF
THE REQUIREMENTS FOR THE DEGREE OF
DOCTOR OF PHILOSOPHY

in the Department
of
Astronomy and Geophysics

We accept this thesis as conforming to the
required standard

THE UNIVERSITY OF BRITISH COLUMBIA
November, 1972

In presenting this thesis in partial fulfilment of the requirements for an advanced degree at the University of British Columbia, I agree that the Library shall make it freely available for reference and study. I further agree that permission for extensive copying of this thesis for scholarly purposes may be granted by the Head of my Department or by his representatives. It is understood that copying or publication of this thesis for financial gain shall not be allowed without my written permission.

Department of Geophysics and Astronomy

The University of British Columbia
Vancouver 8, Canada

Date Jan 18, 1973

ABSTRACT

It is a well-known observational fact that the velocity distribution of a group of stars is related to the spectral classes of the stars. In particular, a large vertex deviation exists for stars of early spectral types, which disappears for stars of later spectral types. Also, the velocity dispersions tend to increase with later spectral types.

An examination of the nearby stars yielded relations between the velocity distribution and the spectral type. Since it was possible to estimate ages for a number of stars, the dependence of the velocity dispersions on age could also be determined.

It was proposed that the observed effects are due to spiral density waves. If account was taken also of the fact that the orbits of the younger stars are not yet well-mixed, then it was found that the predicted values of the vertex deviation agree quite well with the observational values. The increase in the velocity dispersion can be explained if the spiral pattern has dissolved and reformed a number of times. From a comparison of the theoretical age-dependence of the velocity dispersion and the observational curve it was possible to estimate the number of spiral patterns which have existed, their amplitudes and their decay rates.

TABLE OF CONTENTS

ABSTRACT (i)

LIST OF TABLES (iv)

LIST OF FIGURES (v)

ACKNOWLEDGEMENTS (vi)

CHAPTER 1 INTRODUCTION

1.1 The Problem 1

1.2 Review of Previous Work 1

1.3 Scope of the Thesis 8

CHAPTER 2 AN ANALYSIS OF THE OBSERVATIONAL DATA

2.1 Relation of Velocity Distribution to Spectral Type 12

2.2 The Determination of Stellar Ages 17

2.3 Relation of Velocity Distribution to Age 23

CHAPTER 3 THE RESPONSE OF STARS TO A SPIRAL GRAVITATIONAL FIELD

3.1 Changes in the Distribution Function 27

3.2 The Solution of the Amplitude Equation 40

3.3 The Elements of the Velocity Distribution 43

3.4 The Solution of the General Integral 48

3.5 Results 53

CHAPTER 4 COLLISIONLESS RELAXATION IN THE GALAXY

4.1 Introduction 57

4.2 Epicycle Theory 58

4.3 Mathematical Formulation 62

4.4 Results 69

CHAPTER 5 THE VERTEX DEVIATION 72

CHAPTER 6 THE TIME-DEPENDENCE OF THE VELOCITY DISPERSION

6.1 Introduction 77

6.2 Mathematical Formulation 79

6.3 Results 81

CHAPTER 7 CONCLUSIONS 85

BIBLIOGRAPHY 121

LIST OF TABLES

Table		
I	Variation of velocity distribution with spectral type.	87
II	Adjusted velocity distributions.	88
III	Velocity distributions from medians.	89
IV	The zero-age main sequence.	90
V	Age estimates for the evolved stars.	91
VI	Age estimates for the upper main sequence stars.	93
VII	Quality classes.	95
VIII	Cluster ages.	95
IX	Age estimates for the giants.	96
X	Uncertainties in the ages and velocity dispersions.	97
XI	Velocity distributions of the age groups.	98
XIII	Parameters of the spiral pattern.	99
XIV	Comparison of Results.	99
XV	Variation of the mean radial velocity.	100
XVI	Variation of the mean tangential velocity.	100
XVII	Variation of the radial velocity dispersion.	101
XVIII	Variation of the axis ratio.	101
XIX	Variation of the vertex deviation.	102
XX	Variation of the density.	102
XXI	Comparison of angular velocities and epicyclic frequencies.	103

LIST OF FIGURES

Figure		
1	Model tracks from Schlesinger's formulae.	104
2	Isochrones.	105
3	Cluster Composite.	106
4	Age-dependence of the velocity dispersions.	107
5	Time-dependence of radial velocity.	108
6	Time-dependence of tangential velocity.	109
7	Time-dependence of radial velocity dispersion.	110
8	Time-dependence of axis ratio.	111
9	Time-dependence of vertex deviation.	112
10	Time-dependence of radial velocity.	113
11	Time-dependence of tangential velocity.	114
12	Time-dependence of radial velocity dispersion.	115
13	Time-dependence of axis ratio.	116
14	Time-dependence of vertex deviation.	117
15	Relation between velocity dispersion and vertex deviation.	118
16	Age dependence of the radial velocity dispersion.	119
17	Revised Age Dependence of the Radial Velocity Dispersion	120

ACKNOWLEDGEMENTS

It is with pleasure that I acknowledge the invaluable counsel and encouragement of Dr. M.W. Ovenden during the development of this research. I am also grateful to Drs. J.R. Auman, G.A.H. Walker and G.G. Fahlman for helpful discussions and criticisms of various phases of the work. Sincere thanks to Chris Tunstall for a very fine job of typing the thesis. I would also like to express my gratitude to the National Research Counsel which has provided financial support in the form of an N.R.C. Scholarship.

CHAPTER 1

INTRODUCTION

1.1 The Problem

If the Galaxy were in a steady state, the velocity distribution would be expected to be of the Schwarzschild type--an ellipsoid with the vertex pointing towards the galactic centre. It would also be expected that the velocity distribution would be independent of the ages of the stars. In fact, it has been observed that although the velocity distribution does approximate an ellipse, the vertex deviates from the galactic centre. The vertex deviation and the velocity dispersions are observed to be correlated to the spectral classes of the various subpopulations. This appears to imply that the velocity distribution may be related to the ages of the stars. It is the object of this thesis to examine the nearby stars and hence to determine a relation between the velocity distribution and the age. An attempt will then be made to derive an explanation of the observed relation from the theoretical point of view.

1.2 Review of Previous Work

Although the large velocity dispersion of very old stars is almost certainly a relic of the rapid initial

collapse of the early Galaxy, it appears unlikely that the galactic gas disk can have been sufficiently different a few times 10^9 years ago from its present state. It thus seems probable that the velocity dispersions increased after the stars were formed. Some mechanism should then be contained in the galactic system which is capable of producing the observed increase in the velocity dispersion.

It has been shown by Chandrasekhar (1942) that star-star encounters are not satisfactory since the resulting relaxation time is much larger than the accepted age of the Galaxy. Spitzer and Schwarzschild (1953) suggested that random momentum exchanges between large cloud aggregates and individual stars could cause the observed increase in the velocity dispersion. However, Barbanis and Woltjer (1967), find it doubtful that enough massive cloud complexes do exist in interstellar space. Toomre (1964) suggested that gravitational instabilities developing in the galactic disk might be responsible. According to Julian (1967), instabilities that might have some relation to spiral structure would be effective. This treatment is, however, only local and has not been applied to the global spiral pattern.

It was proposed by Marochnik and Suchkov (1969) that the relaxation of the younger stars is due to the

fact that the system of Population I stars rotates faster than the system of Population II stars. Interactions between the two systems cause Landau instabilities which produce density waves. The growing density waves then cause the velocity dispersions to grow. To obtain an increase of the observed magnitude it was required to assume that 90 percent of the stars belonged to Population II and that the system of Population II stars was non-rotating. Observational evidence does not support these assumptions.

Barbanis and Woltjer (1967) have shown that for stars with small peculiar velocities the gravitational action of spiral perturbations which decay exponentially with time can account for the increase in the velocity dispersion. This was done using first-order epicyclic theory. More recently, Pomagaev (1971) approached the problem in a similar manner but expanded the theory to include second-order terms. This approach differed in that he considered the spiral pattern to be growing exponentially. Although it is possible to estimate in this manner the mean velocities due to the spiral waves, the rate at which the velocity dispersion changes with time is difficult to determine even if it is assumed that the stars are well-mixed and that averages are taken over all angles.

Although the vertex deviation has been attributed to the presence of spiral arms, two basically different approaches have been used. In the first, it is assumed that the deviation is a reflection of initial conditions. Stars are formed in the spiral arms and migrate, the influence of small-scale density fluctuations not deleting their memory of origin. According to Woolley (1970) the origin of Gliese's A stars can be traced back to a thin strip resembling a spiral arm. Yuan (1971) also studied the effect of the origin of the stars. He assumed stars were formed in the spiral arms. Then he calculated orbits for a number of hypothetical stars to arrive at a statistical prediction of the velocity distribution at the Sun. For A stars this compared fairly well with observation. However, Yuan also assumed that at formation the stars are in a well-mixed state. This appears to be unlikely.

In the second approach, the deviation is postulated to be caused by a stationary distribution in the presence of the spiral gravitational field. Kalnajs (1971) found that if the spiral field is 5% of the mean gravitational field it is insufficient to produce the observed deviation. Independently, Mayor (1970) showed that under certain conditions such a field could cause the distribution of a group of stars with a small velocity dispersion to be distorted so that it becomes similar to

the observed distribution. However, to do this two assumptions were made--firstly, that the low-dispersion had reached a well-mixed state and secondly, that the Sun is located on the inner edge of a major spiral arm. Whether or not the local spiral arm belongs to the main two-arm pattern is a controversial topic. However, most observations favor the local Orion arm as an inter-arm spur (Simonson (1970)). Even if the local arm were a major arm, the parameters of the density wave would have to be chosen consistently. According to Yuan, a simple re-orientation of Lin's pattern is not permissable.

Recently, a number of authors have considered the Galaxy as consisting of a continuum of stars. The evolution of the system is then studied by using hydrodynamic equations. These are derived from the Boltzmann equation as equations for the first few moments of the distribution function. Since the equation for the n^{th} moment includes a term dependent on the spatial derivative of the $(n+1)^{th}$ moment, the moment equations form an open coupled system. In a small number of special cases the chain of equations can be broken and a closed system of equations is obtained. These cases will be briefly examined below.

(1) If collisions dominate so that one has local "thermodynamic" equilibrium, it is possible to apply the Chapman-Enskog expansion technique (Chapman and Cowling

(1953)). Since in the Galaxy collisions have a negligible effect (Chandrasekhar), this is not applicable.

(2) Marochnik (1964) found that it is possible to obtain a closed set of equations for motion perpendicular to the rotation axis if one is interested in the evolution of the Galaxy over a time-scale very much longer than the period of rotation. He used the method developed by Chew, Goldberger, and Low (1956) who examined the analogous case of a collisionless plasma having a strong magnetic field.

Since this method is not valid for timescales comparable to the rotation period, effects such as orbital mixing cannot be examined. Hence this method limits the description of the evolution of the system to a first-order approximation.

(3) The last case is when the term containing the next higher moment can be neglected. This is true if the spatial variation of the higher moment can be neglected (Hunter (1969)) or if the characteristic velocity of the system is much greater than the velocity dispersion and the next higher moments are small compared to the lower-order moments. The latter is known as the low temperature approximation and is described in more detail by Bernstein and Trehan (1961). This method is valid only if the stellar velocity distribution is at equilibrium. If this is not so, orbital mixing occurs and the spatial derivatives of the moments become very large. It should be

noted that "equilibrium" is used here to denote the state where orbital mixing has been completed and all memory of the origin of the stars has vanished.

In spite of their shortcomings, the hydrodynamic equations have been used with some success. Kato (1968) was able to calculate the form of the velocity ellipsoid if the stars had a systematic mean motion superposed on the circular velocity. This was limited to the steady-state case.

The time variation of the velocity ellipsoid due to star-cloud encounters and due to galactic rotation was examined by Kitamura (1968). Near the Sun, the effect of star-cloud encounters was found to be negligible. Kitamura also found that if initially the vertex deviation or axis ratio were different from the equilibrium values, the velocity ellipsoid would oscillate, without damping, about the equilibrium values. The period of oscillation was $\sim 10^8$ years.

However, Kitamura assumed that the stars had no systematic mean motions in addition to the circular velocity and that third and higher order moments could be neglected. These assumptions are valid only if the velocity distribution is at all times at equilibrium, as is true locally when collisions are frequent. If the

initial velocity distribution is not at equilibrium or if systematic motions do exist, orbital mixing will occur and equilibrium will be approached. The oscillations about equilibrium will hence be damped. The damping is due to the fact that the spatial derivatives of the third and higher moments gradually become dominant because the stars have orbits with differing periods and thus get out of step with each other. Since Kitamura assumes that the initial velocity distribution is not at equilibrium, his assumptions concerning mean motions and third and higher moments are not justified. His hydrodynamic approach is therefore invalid.

In conclusion, it was found that the hydrodynamic equations are applicable only if the velocity distribution is time-independent or if we are interested in the evolution of the system over very large time-scales. Due primarily to the phenomenon of orbital mixing, the method is inadequate for describing the time variation of the velocity ellipsoid caused by small perturbations from equilibrium.

1.3 Scope of the Thesis

Relationships between the velocity distributions and the ages of groups of stars will be determined by examining the nearby stars in Gliese's (1969) catalogue. These stars were selected because their sample is

relatively complete and because their data are more accurate than those for more distant stars. The stars will be divided into groups according to spectral type. For each group the velocity distribution will be then calculated. This will furnish a relation between the velocity dispersion and the vertex deviation. Since the spectral type may be considered to be a rough indicator of age, this will provide also a zeroth-order estimate of the age-dependence of the velocity distribution. Using Iben's (1966) stellar models it is possible to estimate (for a number of stars) their ages from their positions on the color-magnitude diagram. Hence, by dividing the stars into various age groups, the age-dependence of the velocity distribution can be found. This will all be dealt with in Chapter 2.

It is emphasized that the age estimates will have unavoidable uncertainties. However, the importance to this thesis of the derived functional variation of the velocity dispersion with age lies not in the precise details of the function but in the demonstration that the theoretical mechanism through which it is explained is important in the dynamical evolution of the Galaxy.

It is postulated that the observed age-dependence of the velocity distribution is due primarily to the

presence of spiral density waves. Since the density waves proposed by Lin, Yuan and Shu (1969) appear to be supported observationally, the waves are assumed to be of this form. However, Toomre (1969) has found that unless the waves are replenished they will be damped due to interactions with the stars. Harrison (1970) has suggested that spiral waves are generated by the interaction of radial flow from the galactic centre with the galactic rotation flow. The resulting spiral waves trail and are propagated outward. These waves grow or decay exponentially.

In Chapter 3 the response of a sub-population of stars to such density waves will be determined. This will be done for the general case of a velocity ellipsoid with arbitrary axis ratio and vertex deviation. The density waves will be assumed to vary exponentially with time. The results will then be examined to test the sensitivity of the response to the values of the axis ratio and vertex deviation.

If a sub-population of stars initially has a velocity distribution which is not at equilibrium, then the stellar orbits gradually become "mixed" due to differences in orbital periods. As mixing reaches completion, the stars will be said to approach "equilibrium".

In Chapter 4 such collisionless relaxation is studied in detail in order to determine how and how quickly equilibrium is reached. This will make it possible to calculate the axis ratios and vertex deviations (and hence the response of the stars to density waves) for sub-populations of stars which have not yet reached the equilibrium state.

Using the mixing theory and being able to determine the response to density waves, it is now possible to calculate the perturbed velocity distribution of a sub-population whose unperturbed velocity distribution has not reached equilibrium. This will be done in Chapter 5. A theoretical relation between the vertex deviation and velocity dispersion will be obtained and will be compared to the empirical results.

In Chapter 6 the effect of density waves on the velocity dispersion will be examined. The waves will be assumed to have decayed exponentially. Using the methods of Chapter 3, the mean velocity of a sub-population due to the wave can be calculated. As the amplitude of the wave diminishes the mean velocity also diminishes as mixing occurs. The resulting increase in the velocity dispersion can then be easily obtained. Relations between the velocity dispersion and time will then be determined for density waves of various initial amplitudes and decay rates. These will be compared with the empirical curve.

CHAPTER 2

AN ANALYSIS OF THE OBSERVATIONAL DATA

2.1 Relation of Velocity Distribution to Spectral Type

In order that the samples of stars considered be relatively complete, only nearby stars were selected. The stars were all taken from Gliese's (1969) catalogue of nearby stars. Only those within 22 parsecs of the Sun were used. This left 1105 stars having known velocity components, approximately 900 of these having a known (B-V).

The mean velocities and the velocity dispersions were determined from the following formulae, respectively

$$\bar{V} = \frac{1}{n} \sum_{i=1}^{n} V_i \qquad (1)$$

$$\sigma_v^2 = \frac{1}{n-1} \sum_{i=1}^{n} (V_i - \bar{V})^2 \qquad (2)$$

where n is the number of stars in the sample and V_i is the velocity of the i^{th} star. This method of calculating velocity dispersions is unfortunately highly sensitive to stars with larger velocities, giving them an unduly

high weight. Woolley (1958) found that for a Gaussian velocity distribution the velocity dispersion is given by

$$\sigma_v = 1.483 \times \text{median of } (V_i\text{-median velocity}) \qquad (3)$$

He preferred the median to other Gaussian characteristics as it avoids giving high weight to exceptionally high velocities. However, large numbers of stars are needed in this approach. If the number is small and there are few stars with velocities near the average velocity, then the median may differ greatly from the average, causing large errors in σ_v. For groups of stars having large velocities the distribution in v is not Gaussian but asymmetrical--large negative values of v occuring more frequently than equally large positive values. This is due to the fact that stars with large positive v (greater than 65 km/sec) escape from the Galaxy. Hence the significance of σ_v is weakened for the high velocity stars. For groups containing only a small fraction of high velocity stars, the distribution is well approximated by a Gaussian distribution.

The difficulty of stars with large velocities was avoided in the following manner. Using equation (2) the velocity dispersions were calculated for each class of stars. Stars having velocities differing from the mean by more than twice the velocity dispersion were then eliminated.

Having eliminated the high velocity stars, the vertex deviation ℓ was found using the relation

$$\tan 2\ell = \frac{2\sum_{i=1}^{n}(u_i-\bar{u})(v_i-\bar{v})}{\sum(u_i-\bar{u})^2 - \sum(v_i-\bar{v})^2} \qquad (4)$$

where u is the velocity component away from the galactic centre and v is in the direction of rotation. The stars were first divided into spectral classes. In each class the giants, sub-dwarfs and white dwarfs were eliminated. The velocity dispersions were then calculated for each class and the high velocity stars eliminated. The mean velocities, the velocity dispersions and the vertex deviation were then calculated for each group. The results are shown in Tables I and II.

From Table II it is apparent that the kinematic properties of stars are correlated with the spectral type. The phenomenon of asymmetric drift is demonstrated by the change in v. It is, however, primarily a function of the velocity dispersions. The velocity dispersions exhibit a steady growth through the spectral types, reaching their maximums in the white dwarf and sub-dwarf classes. The vertex deviation, on the other hand, has large values for early spectral types and then gradually diminishes. Although Delhaye(1965) has observed much larger vertex deviations for young stars these values are not reproduced here because there are very few early type (O-B)

stars within 22 parsecs of the Sun.

The median velocities and the velocity dispersions obtained by then using equation (3) are listed in Table III. The agreement between Tables II and III is quite good, suggesting that a Gaussian distribution well represents the velocity distribution of the stars. The differences in the various velocity dispersions of the white dwarfs and sub-dwarfs are caused by the small numbers of stars in these samples.

It is emphasized that in the determination of the velocity distributions stars with large velocities were omitted only because the velocity dispersions and the vertex deviation were highly sensitive to such stars. Since the vast majority of the stars were still left, it was still possible to obtain good estimates of the velocity dispersions and the vertex deviation for each group.

Table II conveys the suggestion of equi-partition of energy. By this is meant that the velocity dispersion increases with spectral type simply because the masses of the early-type stars are greater than those of of the stars of later spectral type. However, Woolley (1958) found that when the w-velocity dispersions are

classified according to stellar mass there is no significant variation. Von Hoerner (1960) has found that for stars of spectral type later than G5 no correlation exists between stellar mass and velocity dispersion in the plane. It thus appears unlikely that equi-partition of energy exists here.

It has been shown that the velocity distribution of the nearby stars is related to the spectral type. Since the spectral type may be considered to be a rough indicator of age, this is in fact a zeroth-order estimate of the age dependence of the velocity parameters. A more accurate estimate will be attempted in the next section.

2.2 The Determination of Stellar Ages

To estimate ages of stars from their positions on the colour-magnitude diagram, it was first necessary to determine a number of isochronic lines for the diagram. The age of a star may then be determined by its position relative to these lines. The lines were found by the following procedure.

Iben's (1966) evolutionary stellar model tracks for 1.0, 1.25, 1.5, 2.25 and 3 solar masses were used. These assumed an initial composition of 70.8 percent hydrogen and 27.2 percent helium. Since only a small number of isochronic points could be determined from the five tracks, it was necessary to interpolate between the models. Through such interpolation Schlesinger (1969) has derived some convenient formulae. He finds the zero age main sequence (ZAMS) to be given by

$$\log L = -0.1514 + 5.293M - 1.31 (\log M)^{1.7} \quad (1)$$

$$\log T_e = 3.7486 + 0.678 (\log M)^{0.8} \quad (2)$$

where L is the luminosity, T_e is the effective temperature and M is the mass in solar masses. The hydrogen burning times were found to be

$$\log t_1 = 9.5650 - 3.8075 \log M + 1.31 (\log M)^{1.7} \quad (3)$$

$$\log t_2 = 9.4817 - 4.293 \log M + 1.6312 (\log M)^{1.7} \quad (4)$$

where t_1 is the time needed for half of the initial central hydrogen to be depleted (i.e. from Iben point 1 to 2) and

t_2 is the time needed from there until overall contraction starts (from Iben point 2 to 3). If M is between 1 and 3 solar masses, these relations give log L, log T_e and log t to within 0.03, 0.01 and 0.02 respectively.

The ZAMS thus obtained and the empirical main sequence determined by Johnson (1963) differ significantly. Adapting the method of Sandage and Eggen (1969), the two were reconciled by displacing the theoretical ZAMS horizontally (i.e. in log T_e) to fit the empirical line while keeping the luminosity constant. Justification for such a shifting of the model tracks from the calculated effective temperature comes from Demarque's (1968) demonstration that ages are insensitive to differences in model radii, provided the luminosity is correctly given.

The tables given by Schlesinger were used to convert luminosity and temperature to visual magnitude and (B-V) color. They consisted, in part, of Johnson's (1966) bolometric corrections and the (B-V, T_e) relation due to Harris (1963). A value of 4.72 magnitudes was used for the solar bolometric magnitude. Using equations (1) to (4), model tracks were calculated for stars from 1.0 to 2.5 solar masses at intervals of 0.1 solar mass. These were then adjusted to fit the empirical main sequence (see Table IV). The hydrogen burning times and the starting point on the ZAMS having been determined for each model, the tracks were then plotted on the color-magnitude diagram (Fig. 1)

by interpolating from Iben's model tracks. From the plotted tracks isochrones were drawn by connecting points representing identical ages. The resulting isochrones are shown in Fig 2.

Ages for stars which have evolved far from the main sequence could be estimated by noting their positions on the color-magnitude diagram with respect to the isochrones. Probable errors in the ages were estimated by observing the deviations in the positions caused by the uncertainties in the magnitudes and (B-V) colors. The uncertainty in (B-V) was assumed to be less than 0.02 magnitudes. The uncertainty in the absolute magnitude was taken from Gliese and included the probable error in the parallax. For each star a maximum and a minimum age were estimated. The following assumptions were then made--(1) that the rate of star formation had not changed appreciably between the minimum and maximum age and (2) that the stars in the solar neighbourhood are well-mixed, representing stars of all ages. With these assumptions, the star could have any age between the minimum and maximum with equal probability. Since we are interested in the mean age of a group of stars, the age for each star was estimated by taking the average of the minimum and maximum age. Essentially these assumptions introduce a correlation between age and spectral type.

According to von Hoerner (1960) the rate of star formation has been approximately constant except for the

very old stars. The ages for the very old stars must therefore be weighted accordingly if the minimum and maximum estimates differ greatly. The assumption that the stars are spatially mixed is valid only for stars older than about 10^9 years. Hence, in the final analysis, only the stars older than 10^9 years will be used.

For stars which have not yet evolved far from the main sequence, ages were estimated by determining the positions of the stars with respect to the points on the model tracks corresponding to t_1 and t_2. Stars lying more than one magnitude below the main sequence were discarded. The maximum ages of stars still being below or on the ZAMS were taken to be the corresponding t_1 times. Since the minimum ages, the contraction times, were small, the final age estimates were taken to be half of the t_1 times. This was justified by our assumptions on the rate of star formation. The age estimates for these stars were considerably more uncertain than those for the evolved stars, particularly for the main sequence stars having a (B-V) greater than 0.50 magnitudes. For this reason only those main sequence stars having a (B-V) of less than 0.5 magnitudes were considered.

The estimated ages for the evolved stars and for the upper main sequence stars are listed in Tables V and VI respectively. The first column contains the number of the star given in Gliese's catalogue while the fourth

column lists Q, the quality of the magnitude. The values of Q and the corresponding uncertainty ranges are listed in Table VII.

Age estimates for the giants were obtained by using a composite of galactic cluster sequences. A comparison of the cluster sequences and the previously determined isochrones (Fig. 2) provided estimates of the cluster ages. The ages of the giants could then be calculated by noting their positions with respect to the cluster sequences.

The cluster sequences which were used to form the composite (Fig. 3) were those drawn by Sandage and Eggen. In Table VIII, age estimates are given for the clusters. Our estimates for NGC 188 and M 67 agree quite well with those of Sandage and Eggen and Iben. However, our values are consistently much larger than Lindoff's (1968) estimates. This is partly due to the fact that Lindoff used the tables in Allen (1963) to convert (L, T_e) to $(M_v, B-V)$. These tables, outdated, are inferior to those of Schlesinger. More important, Lindoff had not adjusted his theoretical ZAMS to fit the empirical ZAMS. Since they differ significantly, this would cause large differences in the resulting age estimates. The isochrones of Sandage and Eggen yielded age estimates of NGC 3680 and NGC 7789 which were similar to ours. A comparison of the results of Harris and Schlesinger suggested that the uncertainties in converting (L,T_e) to $(M_v, B-V)$ were no greater than $(0^m.05, 0^m.01)$.

From the composite in Fig. 3 it can be seen that at certain places the sequences come very near to each other, at some points even crossing. At those positions it is extremely difficult to arrive at accurate age estimates. Small uncertainties in the magnitudes or colors cause very large probable error in the ages then. Hence it was not possible to obtain ages for all of the giants. Estimates for the ages of the giants are given in Table IX.

Due to low metal content, the subdwarfs lie about one magnitude below the normal ZAMS. If the metal content of the original interstellar material were negligible and if the timescale for homogeneous mixing of the interstellar medium is short compared to the age of the Galaxy, then the subdwarfs must belong to the very oldest stars.

The giants and the upper main sequence stars are all relatively bright and thus their samples can be assumed to be almost complete. The subdwarfs, however, are quite faint and selection effects can easily give rise to a biased sample. The most important selection effect, according to Von Hoerner (1960) is the magnitude effect. Faint stars are difficult to observe and are put on observing lists only if they have noticeably high proper motions. Thus, on the average, the faint stars are expected to show higher velocities. Opposing this is the quality effect.

Stars whose parallaxes have been overestimated will appear to lie below the main sequence. However, if the parallax has been overestimated the space velocity will be reduced. Hence this effect tends to give stars lower velocities.

The subdwarfs were selected by considering all stars with (B-V) greater than 1.2 magnitudes and lying at least one magnitude below the ZAMS. For very faint stars the main sequence of Gliese (1968) was used. Since Gliese (1956) has shown that emission stars do not exhibit a dependence on spectral type and that they have smaller velocities that is normal, stars with emission spectra were omitted. To minimize the quality effect, only stars of quality classes (Q) 1, 2 and 3 were used. Finally, in order to reduce the magnitude effect, only stars whose velocities differed from the mean velocities by no more than twice the standard deviation for the class were considered. This left only 18 subdwarfs.

From their relative positions with respect to the isochrones, the oldest evolved stars appeared to be about 12×10^9 years old. Hence this was taken to be the age of the subdwarfs.

2.3 Relation of Velocity Dispersion to Age

The stars whose ages had been estimated were then divided into a number of groups corresponding to

various age ranges. The subdwarfs and white dwarfs were considered separately. For each group the velocity distribution was determined by using equations (1) and (2) of section 2.1 again. The mean age was also calculated for each group but since each individual age had an uncertainty due to inaccuracies in the star's magnitude and color, the mean age likewise had a probable error. This uncertainty, σ, was found using the relation

$$\sigma^2 = \frac{\sum_{i=1}^{n} \sigma_i^2}{n} \qquad (1)$$

where n is the number of stars and σ_i is the uncertainty in the age of the i^{th} star.

The probable errors in the velocity dispersions were estimated by assuming the samples to be from Gaussian populations and then calculating 70% confidence intervals. Our samples were too small to obtain reasonable estimates of the vertex deviations. The uncertainties are summarized in Table X.

The components of the velocity distribution for each group are listed in Table XI. Although u and w appear to vary irregularly with age, v increases steadily in magnitude (asymmetric drift). The velocity dispersions, in all three directions, also increase with age. This may be seen more clearly in Fig. 4. Error bars have added

to only the radial velocity dispersion since they will be similar to the error bars for the other dispersions. It appears as if the curves could be divided into two intervals. Until an age of about 2.5×10^9 years there is a rather rapid increase,but from there on the increase continues more slowly.

Once stars have become well-mixed they approach an "equilibrium" velocity distribution. Hence for older stars it can be assumed that, after correcting for the influence of the spiral arms, the velocity distribution is near equilibrium. If the velocity distribution is at equilibrium, the ratio of the velocity dispersions, σ_u^2/σ_v^2 , will equal 0.4 at the Sun. From Table II it can be seen that for $\sigma_v \sim 20$ km/sec equilibrium is already approached.

The theory that will be developed can of course be applied to any function of age and velocity dispersion derived from observations. However, the actual variation of velocity dispersion with age derived here will be simply interpreted by the theory. The significance of the theory is not dependent on minor re-interpretations of the data.

The age estimates are, admittedly, subject to a number of uncertainties due to the assumptions regarding star formation rates, stellar composition and the evolutionary tracks, among others. This is true particularly for stars near the main sequence where the assumptions about star formation rates become important. Here we have relied heavily on von Hoerner's results which indicated an almost constant rate of star formation over the last $\sim 6 \times 10^9$ years. This clearly injects an age-dependence on the spectral type for main sequence stars. Hopefully, the uncertainties may be reduced in the future. It is felt, however, that the age estimates cannot be greatly improved upon with the presently available data.

CHAPTER 3

THE RESPONSE OF STARS TO A SPIRAL GRAVITATIONAL FIELD

3.1 Changes in the Distribution Function

The response of a stellar disk sub-population to a spiral gravitational field will now be examined. In the initial stages of development the procedure will resemble that of Lin, Yuan and Shu (1969) and Mayor (1970). We have borrowed freely from these sources. However, whereas Lin and Mayor considered only the case of a well-mixed ("equilibrium") sub-population in a time-independent spiral field, we shall examine the more general case where the stars need not be well-mixed and the spiral field may change with time.

Let r represent the distance from the galactic center and let θ be the angular displacement measured clockwise from the galactic radius passing through the Sun. The galactic co-ordinates of a star are then given by (r,θ). For an infinitesimally thin disk the collisionless Boltzmann equation in such a co-ordinate system is given by

$$\frac{\partial f}{\partial t}+\Pi_1\frac{\partial f}{\partial r}+\Theta_1\frac{\partial f}{\partial \theta}+\left(\frac{\partial U}{\partial r}+\frac{\Theta_1^2}{r}\right)\frac{\partial f}{\partial \Pi_1}+\left(\frac{1}{r}\frac{\partial U}{\partial \theta}-\frac{\Pi_1\Theta_1}{r}\right)\frac{\partial f}{\partial \Theta_1}=0 \qquad (1)$$

where f is the distribution function, U is the gravitational

field and (Π_1, Θ_1) are the components of the total stellar velocity. If Ω is the angular velocity of the circular motion defined by balancing the centrifugal acceleration $r\Omega^2$ with the symmetrical gravitational field and if the peculiar velocity components of the centroid are given by (Π_0, Θ_0), then the velocity components relative to the centroid velocity are

$$\Pi = \Pi_1 - \Pi_0 \tag{2}$$

$$\Theta = \Theta_1 - \Theta_0 - r\Omega \tag{3}$$

Since the centroid velocity components are, in general, small compared to (Π, Θ) they will be neglected. This reduces equations (2) and (3) to

$$\Pi = \Pi_1 \tag{4}$$

$$\Theta = \Theta_1 - r\Omega \tag{5}$$

In order to transform the Boltzmann equation to (Π, Θ), the following relations are needed:

$$\frac{\partial f}{\partial \Theta} = \frac{\partial f}{\partial \Theta_1} \tag{6}$$

$$\frac{\partial f}{\partial \Pi} = \frac{\partial f}{\partial \Pi_1} \tag{7}$$

$$\frac{\partial f}{\partial r} = \frac{\partial f}{\partial r} + \frac{\partial f}{\partial \Theta}\frac{\partial \Theta}{\partial r} \tag{8}$$

The last equation becomes

$$\frac{\delta f}{\delta r} = \frac{\partial f}{\partial r} - \left(\Omega + r\frac{\partial \Theta}{\partial r}\right)\frac{\partial f}{\partial \Theta} \qquad (9)$$

Equation (1) may now be rewritten as

$$\frac{\partial f}{\partial t} + \frac{\partial f}{\partial r} + \left(\Omega + \frac{\Theta}{r}\right)\frac{\partial f}{\partial \theta} + \left(\frac{\partial U}{\partial r} + r\Omega^2 + 2\Omega\Theta + \frac{\Theta^2}{r}\right)\frac{\partial f}{\partial \Pi} + \left(\frac{1}{r}\frac{\partial U}{\partial \theta} - \kappa^2 \frac{\Pi\Theta}{r}\right)\frac{\partial f}{\partial \Theta} = 0 \qquad (10)$$

where K, the epicyclic frequency, is defined by

$$\kappa^2 \equiv 4\Omega^2\left(1 + \frac{r}{2}\frac{\partial \Omega}{\partial r}\right) \qquad (11)$$

Suppose that U consists of a symmetrical gravitational field U_o upon which is superimposed a spiral gravitational field U_1 of the form

$$U_1 = A(r,t)\exp\left[i(mwt - m\theta + \Phi(r)\right] \qquad (12)$$

where A defines the amplitude of the pattern, n is the number of arms, Φ represents the phase and w is the relative angular velocity of the pattern. The spiral is then defined by lines of constant phase through the relation

$$n(\theta - \theta_o) = \Phi(r) - \Phi(r_o) \qquad (13)$$

where (r_o, θ_o) is the initial reference position. Lin defines the phase term as

$$\Phi(r) - \Phi(r_o) = \frac{m}{\tan i}\ln\frac{r}{r_o} \qquad (14)$$

where i is the inclination of the pattern.

Since the radial derivative of U_o is given by $-r\Omega^2$, equation (10) becomes, on substituting $U_o + U_1$ for U,

$$\frac{\partial f}{\partial t}+\Pi\frac{\partial f}{\partial r}+(\Omega+\frac{\Theta}{r})\frac{\partial f}{\partial \theta}+(\frac{\partial U_1}{\partial r}+2\Omega+\frac{\Theta^2}{r})\frac{\partial f}{\partial \Pi}+(\frac{1}{r}\frac{\partial U_1}{\partial \theta}-\frac{\Pi k^2}{2\Omega}-\frac{\Pi}{r})\frac{\partial f}{\partial \Theta}=0 \qquad (15)$$

For convenience, the left-hand side of this equation will be written symbolically as $L(f)$. If only a symmetric field exists (i.e. $U_1=0$) it will be written as $L_o(f)$.

Let f_o be the distribution function which the stars would have had if no spiral field existed. The addition of a spiral field will result in a perturbation ψf_o in the distribution function. It is our aim to determine an expression for ψ. A knowledge of ψ makes it possible to then calculate the perturbations in the components of the velocity distribution. The perturbed distribution function f is given by

$$f = f_o(1+\psi) \qquad (16)$$

Assume that f_o is of the form

$$f_o = c(\theta,r,t)\exp\left[-Q(\theta,r,t,\Theta,\Pi)\right] \qquad (17)$$

On substituting equations (16) and (17) into equation (15),

we then obtain

$$L_o(\psi) = -L_1(\psi) + (1+\psi)L_1(Q) \qquad (18)$$

where $$L_1(\ ) = \frac{\partial U_1}{\partial r}\frac{\partial(\ )}{\partial \Pi} + \frac{1}{r}\frac{\partial U_1}{\partial \theta}\frac{\partial(\ )}{\partial \Theta} \qquad (19)$$

Now, if ψ is small, equation (18) may be linearized to become

$$L_o(\psi) \simeq L_1(Q) \qquad (20)$$

If the spiral field components are of the form described by equation (12), then it is naturally expected that ψ has a similar form;

$$\psi = \phi\ (r,\Pi,\Theta)\exp\left[\, i(mwt - m\Theta + \Phi(r))\right] \qquad (21)$$

where ϕ defines the amplitude of ψ.

Lin has shown that solutions of this form are possible. Mayor, however, has found that the linear approximation is no longer valid if the spiral field is large or if the velocity dispersions of the stars are small. Hence non-linear terms must be included. From equation (18) it is evident that the first non-linear effects associated with a perturbation of type (12) will appear as terms proportional to

$$\exp\left[\, 2i(mwt - m\Theta + \Phi)\right] \qquad (22)$$

The non-linear effects will therefore be estimated by assuming U_1 and ψ have the forms

$$U_1 = \sum_{j=1}^{\infty} b_j(r,t)\ \exp\left[ij(mwt-m\Theta+\Phi)\right] \tag{23}$$

$$\psi = \sum_{k=1}^{\infty} a_k(r,t,\Pi,\Theta)\exp\left[ik(mwt-m\Theta+\Phi)\right] \tag{24}$$

If these are substituted into equation (18) it is found that

$$L_o(a_k)+ika_k\left(-m\frac{\Theta}{r}+mw+\frac{\partial\Phi}{\partial r}\right) = \bar{L}_{1k}(Q)+\sum_{n,j}\left[a_n\bar{L}_{1j}(Q)-\bar{L}_{1n}(a_j)\right]\delta_{k\ j+n} \tag{25}$$

where $\sum_{n,j}$ indicates summation over all values of n and j, δ_{ij} is the Kronecker delta, and

$$L_{ij}(\ ) = -\left(ijb_j\frac{\partial\Phi}{\partial r}+\frac{b_j}{r}\right)\frac{\partial(\ )}{\partial\Pi}+\frac{ijm}{r}b_j\frac{\partial(\ )}{\partial\Theta} \tag{26}$$

Equation (25) may be simplified somewhat by introducing a change of variables, from (Π,Θ) to (T,ℓ). These are related as follows:

$$\Theta = V_2 T\sin\ell \tag{27}$$

$$\Pi = V_1 T\cos\ell \tag{28}$$

where

$$V_1 = \frac{2\Omega^2 r}{k} \tag{29}$$

$$V_2 = r\Omega \tag{30}$$

With this transformation the derivatives, in terms of the new variables, become

$$\frac{\partial(\ )}{\partial \Pi} = \frac{\partial T}{\partial \Pi}\frac{\partial(\ )}{\partial T} + \frac{\partial \ell}{\partial \Pi}\frac{\partial(\ )}{\partial \ell} \tag{31}$$

$$\frac{\partial(\ )}{\partial \Theta} = \frac{\partial T}{\partial \Theta}\frac{\partial(\ )}{\partial T} + \frac{\partial \ell}{\partial \Theta}\frac{\partial(\ )}{\partial \ell} \tag{32}$$

$$\frac{\partial(\ )}{\partial r} = \frac{\partial(\ )}{\partial r} + \frac{\partial T}{\partial r}\frac{\partial(\ )}{\partial T} + \frac{\partial \ell}{\partial r}\frac{\partial(\ )}{\partial \ell} \tag{33}$$

Using relations (27) and (28), equations (31)-(33) may be rewritten

$$\frac{\partial(\ )}{\partial \Pi} = \frac{1}{V_1}\left[\cos\ell\,\frac{\partial(\ )}{\partial T} - \frac{\sin\ell}{T}\frac{\partial(\ )}{\partial \ell}\right] \tag{34}$$

$$\frac{\partial(\ )}{\partial \Theta} = \frac{1}{V_2}\left[\sin\ell\,\frac{\partial(\ )}{\partial T} + \frac{\cos\ell}{T}\frac{\partial(\ )}{\partial \ell}\right] \tag{35}$$

$$\frac{\partial(\ )}{\partial r} = -\frac{T}{2}\frac{\partial \ln(V_1^2+V_2^2)}{\partial r}\frac{\partial(\ )}{\partial T} + \left[\frac{\tan\ell}{2}\frac{\partial \ln(V_1^2+V_2^2)}{\partial r} - \frac{1}{V_2}\frac{\partial V_2}{\partial r}\right]\frac{\partial(\ )}{\partial \ell} + \frac{\partial(\ )}{\partial r} \tag{36}$$

Assuming that the residual velocities Π and Θ are small compared to the circular velocity and ignoring second-order terms, the operator of equation (26) becomes

$$L_{ij}(\ ) = \left[-c_{ij}\cos\ell + \frac{ijmb_j}{V_2}\sin\ell\right]\frac{\partial(\ )}{\partial T} + \frac{\left[c_{ij}\sin\ell + \dfrac{ijmb_j\cos\ell}{V_2}\right]}{T}\frac{\partial(\ )}{\partial \ell} \tag{37}$$

and

$$L_o(\ ) = \frac{\partial(\ )}{\partial t} + \frac{\partial(\ )}{\partial r} - k\frac{\partial(\ )}{\partial \ell} \tag{38}$$

The system (25) may now be rewritten as

$$\frac{\partial a_k}{\partial t}+\frac{\partial a_k}{\partial r}-\frac{k\partial a_k}{\partial \ell}+ika_k\left[mw-2\Omega+\left(\frac{2\Omega^2 r}{k}\right)\left(\frac{\partial \bar{\Phi}}{\partial r}\right)+\cos\ell\right] = S_k(T,\ell) \qquad (39)$$

where

$$S_k = L_{1k}(Q)+\sum_{j,n}\left[a_j L_{1n}(Q)-L_{ij}(a_n)\right]\delta_{k,j+n} \qquad (40)$$

If a_k changes only slowly with r then equation (39) may be further simplified to

$$K^{-1}\frac{\partial a_k}{\partial t}-\frac{\partial a_k}{\partial \ell}+ik\left[\nu+\alpha T\cos\ell\right]\ a_k = K^{-1}S_k \qquad (41)$$

where

$$\nu = \frac{mw-2\Omega}{k} \qquad (42)$$

and

$$\alpha = \frac{2\Omega^2 r}{k}\frac{\partial \bar{\Phi}}{\partial r} \qquad (43)$$

We now depart from Lin and Mayor and continue as follows. To solve equation (41) it is necessary first to specify the variation of U_i with time. Knowing the dependence of the b_j's (the amplitude of U_i) on time, one could then apply a Laplace transform and reduce equation (41) to a differential equation in one variable, ℓ. In certain cases it is possible to use a more direct approach. For example, if the partial differential equation is of the form

$$a + \frac{1}{K}\frac{\partial a}{\partial t} - \frac{\partial a}{\partial \ell} = g(\ell)h(t) \qquad (44)$$

and if the right hand side can be rewritten in the form

$$g(\ell)h(t) = g_1(\ell)h_1(t+\frac{\ell}{K}) \tag{45}$$

where g,h,h_1 and g_1 are arbitrary functions, then if the solution of

$$a - \frac{\partial a}{\partial \ell} = g_1(\ell) \tag{46}$$

is

$$a(\ell) = g_2(\ell) \tag{47}$$

the solution equation (44) is

$$a(\ell,t) = g_2(\ell)h_1(t+\frac{\ell}{K}) \tag{48}$$

This result holds for all functions h(t) which are of the form

$$h(t+\frac{\ell}{K}) = h_1(t)h_2(\ell) + h_3(\ell) \tag{49}$$

If it is assumed that the amplitudes b_j vary either exponentially or sinusoidally, this may be represented by

$$b_j = b_{1j}\exp(\beta t) \tag{50}$$

where β is inversely proportional to the timescale of spiral persistence and is real for exponential changes and imaginary for sinusoidal variations. It is evident that for such functions condition (49) holds. Since equations (37) and

(40) show S_k to be proportional to b_j, S_k may be written as

$$S_k = g(\ell)\exp(\beta t) \tag{51}$$

To satisfy equation (45), S_k is rearranged as

$$S_k = g(\ell)\exp(\frac{-\beta\ell}{K})\ \exp\left[\beta(t+\frac{\ell}{K})\right] \tag{52}$$

Hence, instead of solving equation (41), only the following simplified equation need be solved:

$$\frac{\partial a_k}{\partial \ell} + \phi\, a_k = h_k \tag{53}$$

where

$$\phi = -iK(U + \alpha T\cos\ell\ )$$

$$h_k = -S_k\exp\left[-\beta(t+\frac{\ell}{K})\right]$$

Equation (53) has the solution

$$a_k = \exp\left[-\int\phi\, d\ell\right]\left(c_k + \int_0^{\ell} h_k\exp\left[\int\phi\, d\ell\right] d\ell\right) \tag{54}$$

where c_k is an integration constant.
Since a_k will be periodic in ℓ,

$$a_k(\ell) = a_k(\ell+2\pi) \tag{55}$$

From equations (54) and (55) it is possible to determine c_k, which was found to be given by

$$c_k = \frac{\exp\left[-\int \phi \, d\ell\right]}{1-\exp\left[-\int \phi \, d\ell\right]} \int_0^{2\pi} h_k \exp\left[\int \phi \, d\ell\right] d\ell \qquad (56)$$

From the definitions of ϕ, h and c_k, equation (54) may now be rewritten as

$$a_k = \frac{\gamma_1}{K} \exp\left[\beta t + \frac{\beta \ell}{K}\right] \left[\int_0^{\ell} \frac{h_k}{\gamma_1} d\ell + \frac{\gamma_2}{1-\gamma_2} \int_0^{2\pi} \frac{h_k}{\gamma_1} d\ell\right] \qquad (57)$$

where

$$\gamma_1 = \exp\left[ik(\nu\ell + \alpha\tau \sin\ell)\right]$$

$$\gamma_2 = \exp\left[2\pi(ik\nu + \frac{\beta}{K})\right]$$

If k=1 we have the linear approximation. For the non-linear case only the first two terms are important. Hence only h_1 and h_2 are needed. These were found to be as follows:

$$h_1 = -L_{11}(Q) \exp\left[-\beta(t+\frac{\ell}{K})\right] \qquad (58)$$

$$h_2 = -\left[L_{12}(Q) + a_1 L_{11}(Q) - L_{11}(a_1)\right] \exp\left[-\beta(t+\frac{\ell}{K})\right] \qquad (59)$$

To solve equation (57) it is necessary first to determine the distribution function f_o. For a two-dimensional, ellipsoidal distribution it can easily be shown that the distribution function may be written as

$$f_o = c \exp(-x_1 \Pi^2 - x_2 \Theta^2 - 2x_3 \Pi\Theta) \qquad (60)$$

where c, x_1, x_2, and x_3 are defined as follows

$$c = \frac{\rho_o (x_1 x_2 - x_3^2)^{\frac{1}{2}}}{\pi} \tag{61}$$

$$x_1 = \frac{\sigma_\odot^2}{2\sigma_\odot^2\sigma_\pi^2 - 2\sigma_{\odot\pi}^2} \tag{62}$$

$$x_2 = \frac{x_1\sigma_\pi^2}{\sigma_\odot^2} \tag{63}$$

$$x_3 = \frac{-x_1\sigma_{\odot\pi}^2}{\sigma_\odot^2} \tag{64}$$

Here ρ_o is the star density.

If the transformation defined by equations (27) and (28) is now made equation (60) becomes

$$f_o = c \exp(-T^2(x_1V_1\cos^2\ell + x_2V_2^2\sin^2\ell + 2x_3V_1V_2\cos\ell\sin\ell)) \tag{65}$$

The new parameters p, q and ϕ are now introduced by the relations

$$p\cos\phi = 0.5(x_1V_1^2 - x_2V_2^2) \tag{66}$$

$$p\sin\phi = x_3V_1V_2 \tag{67}$$

$$q = 0.5(x_1V_1^2 + x_2V_2^2) \tag{68}$$

Using trigonometric relations, equation (65) may be rewritten

$$f_o = c \exp(-T^2(q + p\cos(2\ell - \phi))) \tag{69}$$

The expression in the exponential corresponds to the Q introduced in equation (17). To solve equation (57) it is necessary first to determine h_1 and h_2, and hence $L_{ij}(Q)$. Since by its definition (equation (37)) L_{ij} is dependent on the terms $\frac{\partial Q}{\partial T}$ and $\frac{\partial Q}{\partial \ell}$, these will be derived first. From equation (69)

$$Q = -T^2(q + p\cos(2\ell - \phi)) \tag{70}$$

Differentiating Q_1 it is found that

$$\frac{\partial Q}{\partial T} = \frac{2Q}{T} \tag{71}$$

$$\frac{\partial Q}{\partial \ell} = T^2\left[(x_1V_1^2 - x_2V_2^2)\sin 2\ell - 2x_3V_1V_2\cos 2\ell\right] \tag{72}$$

If these expressions are now substituted in equation (37), it follows that

$$L_{ij}(Q) = B_{ij}T\cos\ell + B_{ij}T\sin\ell \tag{73}$$

where

$$B_{1j} = -2x_1V_1\left(ijb_j\frac{\partial\Phi}{\partial r}T + \frac{\partial b_j}{\partial r}\right) + \frac{4ijb_jx_3V_1}{r} \tag{74}$$

$$B_{2j} = -2x_3V_2\left(ijb_j\frac{\partial\Phi}{\partial r}T + \frac{\partial b_j}{\partial r}\right) + \frac{4ijb_jx_2V_2}{r} \tag{75}$$

With these relations it is now possible to determine h_1 and h_2 and hence a_1 and a_2. We shall now proceed to determine a solution for the amplitude equation, equation (57).

3.2 The Solution of the Amplitude Equation

The linear case will first be considered. From equation (57) of section 3.1 it is clear that the amplitude a_1 is given by the relation

$$a_1 = Y_1 \exp\left(\frac{\beta l}{K}\right)\left[\int_0^{l} \frac{h_1}{Y_1} dl + \frac{Y_2}{1-Y_2} \int_0^{2\pi} \frac{h_1}{Y_1} dl\right] / K \qquad (1)$$

where

$$Y_1 = \exp\left[i(\nu l + 2T\sin l)\right]$$

$$Y_2 = \exp\left[2\pi i\left(\nu + \frac{\beta}{K}\right)\right]$$

$$h_1 = (B_{11}T\cos l + B_{21}T\sin l)\exp\left[-\beta\left(t+\frac{l}{K}\right)\right]$$

It is evident that a singularity exists when Y_2 equals unity. For a time-independent wave (i.e. $\beta = 0$) this implies that

$$\nu = \frac{mw - 2\Omega}{K} = \pm n \qquad (2)$$

Hence the singularity occurs when

$$w = \frac{\pm nK + 2\Omega}{m} \qquad (3)$$

If the spiral pattern has two arms (i.e. $m=2$), the singularities at $n=\pm 1$ occur when

$$w = \Omega \pm \frac{K}{2} \qquad (4)$$

These correspond to the Lindblad resonances. Because of the very large resulting amplitudes, the linear approximation is no longer valid at the resonance points. We shall, therefore, limit the development to situations far away from the resonances. Since the Sun is, fortunately, not near a resonance position, such a treatment will be adequate for stars in the local vicinity.

The form of h_1 may be simplified somewhat by using the relations

$$\cos \ell = \frac{\exp(i\ell) + \exp(-i\ell)}{2} \tag{5}$$

$$\sin \ell = -i\frac{\exp(i\ell) - \exp(-i\ell)}{2} \tag{6}$$

The equation for h_1 then becomes

$$h_1 = T \exp(-\beta t + \frac{\beta \ell}{K}) \; A_1 \exp(i\ell) + A_2 \exp(-i\ell) \tag{7}$$

where

$$A_1 = \frac{B_{11} + iB_{21}}{2} \tag{8}$$

$$A_2 = \frac{B_{11} - iB_{21}}{2} \tag{9}$$

To solve the integrals in equation (1) it is convenient to use Bessel functions. The following relation is given by Watson:

$$\exp(-i\alpha T \sin \ell) = \sum_{n=-\infty}^{\infty} J_n(\alpha T) \exp(-in\ell) \tag{10}$$

where $J_n(\alpha T)$ is the Bessel function defined by

$$J_m(\alpha T) = \sum_{m=0}^{\infty} \frac{(-1)^n (\alpha T/2)^{n+2m}}{n!(n+m)!} \tag{11}$$

Substituting equations (7) and (10) into equation (1), the first integral becomes

$$-\int_0^{\ell} T\, A_1 \left[\exp(i\ell) + A_2 \exp(-i\ell)\right] \sum_{n=-\infty}^{\infty} J_n(\alpha T)\, \exp\left[(in-e_1)\ell\right] d\ell \tag{12}$$

where

$$e_1 = i\nu + \frac{\beta}{K} \tag{13}$$

This expression can be easily integrated and becomes

$$T \sum_{n=-\infty}^{\infty} J_n(\alpha T)\left[A_3 \exp(-\left[e_1+in-i\right]\ell) + A_4 \exp(-\left[e_1+in+i\right]\ell) - A_3 - A_4\right] \tag{14}$$

where

$$A_3 = \frac{A_1}{e_1 + in - i} \tag{15}$$

$$A_4 = \frac{A_2}{e_1 + in + i} \tag{16}$$

Similarly, the second integral in equation (1) may be integrated to yield

$$T \sum_{n=-\infty}^{\infty} J_n(\alpha T)\left[A_3+A_4\right]\left[\exp(-2\pi e_1) - 1\right] \tag{17}$$

since

$$\exp(in2\pi) = 1 \tag{18}$$

for all values of n.

If expressions (14) and (17) are now substituted into equation (1), a number of terms disappear. The following simplified relation is left:

$$a_1 = T\exp(\beta t + i\alpha T\sin\ell)\sum_{n=-\infty}^{\infty} J_n(\alpha T)\frac{A_3\exp(i\ell - in\ell) + A_4\exp(-i\ell(1+n))}{K} \tag{19}$$

In the linear approximation, the distribution function is given by

$$f = f_o(1 + a_1\exp[i(mwt - m\theta + \Phi)]) \tag{20}$$

Since an expression for a_1 has now been obtained, it will be possible to solve equation (20) for f.

3.3 The Elements of the Velocity Distribution

A knowledge of the change in the distribution function due to a spiral density wave makes it possible to determine the corresponding changes in the velocity distribution. The perturbations in the star density, the mean velocities and the velocity dispersions are of prime interest.

Let ρ_o denote the star density in the absence of an asymmetric gravitational field. With the addition of a spiral field the perturbed density, ρ, becomes

$$\rho = H(1) \tag{1}$$

where H is an operator defined by

$$H(x) = \int_{-\infty}^{\infty}\int_{-\infty}^{\infty} x f(\Pi,\Theta)\, d\Pi d\Theta$$

Similarly, the mean velocities and the velocity dispersions may be written as

$$\bar{\Pi} = \frac{H(\Pi)}{\rho} \tag{2}$$

$$\bar{\Theta} = \frac{H(\Theta)}{\rho} \tag{3}$$

$$\sigma_{\Pi}^2 = \frac{H(\Pi^2)}{\rho} - \bar{\Pi}^2 \tag{4}$$

$$\sigma_{\Theta}^2 = \frac{H(\Theta^2)}{\rho} - \bar{\Theta}^2 \tag{5}$$

$$\sigma_{\Theta\Pi}^2 = \frac{H(\Theta\Pi)}{\rho} - \bar{\Theta}\bar{\Pi} \tag{6}$$

As was noted in the previous section, the distribution function f is given by

$$f = f_o(1 + a_1 g_1) \tag{7}$$

where

$$g_1 = \exp\left[i(mwt - m\theta + \Phi)\right] \tag{8}$$

If the form of f_o is taken to be that of equation (69) in section 3.1, equation (7) becomes

$$f = cg_2(1 + a_1 g_1) \tag{9}$$

where

$$g_2 = \exp\left[-T^2(q + p\cos(2\ell-\phi))\right] \tag{10}$$

However, if this form of f_o is used then the variables Π and Θ must be transformed to expressions in T and ℓ. Recall that

$$\Pi = V_1 T \cos\ell \tag{11}$$

$$\Theta = V_2 T \sin\ell \tag{12}$$

If equations (1) to (6) are to be integrated over T and ℓ rather than Π and Θ, then the following relation must be used:

$$\int_{-\infty}^{\infty}\int_{-\infty}^{\infty} f(\Pi,\Theta)d\Pi d\Theta = \int_0^{\infty}\int_0^{2\pi} f(T,\ell)\left|\left(\frac{\partial\Pi}{\partial T}\frac{\partial\Theta}{\partial\ell}\right) - \left(\frac{\partial\Pi}{\partial\ell}\frac{\partial\Theta}{\partial T}\right)\right| d\ell\, dT \tag{13}$$

Using equations (11) and (12), the right-hand side reduces to

$$\int_0^{\infty}\int_0^{2\pi} f(T,\ell)TV_1V_2 dT d\ell \tag{14}$$

Substituting equation (9) and (14), equation (1) may be rewritten as

$$\rho = V_1V_2c_o\int_0^{\infty}\int_0^{2\pi} Ta_1g_1g_2 d\ell dT + \rho_o \tag{15}$$

Expressions for the mean velocities and the velocity dispersions can be obtained in a similar fashion. All the resulting equations will have terms containing combinations

of $\cos\ell$ and $\sin\ell$ after substituting for Π and Θ. The integration of the equations can be simplified slightly if the following identities are used again:

$$\cos\ell = \frac{\exp(i\ell) + \exp(-i\ell)}{2} \tag{16}$$

$$\sin\ell = -i\frac{\exp(i\ell) - \exp(-i\ell)}{2} \tag{17}$$

On substituting equation (19) of section 3.2 for a_1 in the equations, it was found that, in general, the following integral must be evaluated:

$$I_z(\lambda,y) = \int_0^{\infty}\int_0^{2\pi} g_2 T\lambda \sum_{n=-\infty}^{\infty} J_n(\alpha T) A_z \exp\left[-i\ell(n-y)+i\alpha T\sin\ell\right] d\ell\, dT \tag{18}$$

where z,λ and y are integers.

In terms of integrals of this form, the components of the velocity distribution may be written as

$$\rho = cV_1V_2g_1\exp(\beta t)\frac{I_3(1,1) + I_4(1,-1)}{K} \tag{19}$$

$$\bar{\Pi} = cV_1^2V_2g_1\exp(\beta t)\frac{I_3(2,2) + I_4(2,-2) + I_3(2,0) + I_4(2,0)}{2K\rho} \tag{20}$$

$$\bar{\Theta} = -icV_1V_2^2g_1\exp(\beta t)\frac{I_3(2,2) - I_4(2,-2) - I_3(2,0) + I_4(2,0)}{2K\rho} \tag{21}$$

$$\sigma_{\pi}^2 = cV_1^3V_2g_1\exp(\beta t)\frac{I_3(3,3)+I_4(3,1)+I_3(3,-1)+I_4(3,-3)+2I_3(3,1)+}{4K\rho}$$

$$\frac{2I_4(3,-1)}{4K\rho} - \bar{\Pi}^2 \qquad (22)$$

$$\sigma_{\Theta}^2 = -cV_1V_2^3g_1\exp(\beta t)\frac{I_3(3,3)+I_4(3,1)+I_3(3,-1)+I_4(3,-3)-2I_3(3,1)-}{4K\rho}$$

$$\frac{2I_4(3,-1)}{4K\rho} - \bar{\Theta}^2 \qquad (23)$$

$$\sigma_{\Theta\pi}^2 = -icV_1^2V_2^2g_1\exp(\beta t)\frac{I_3(3,3)+I_4(3,1)-I_3(3,-1)-I_4(3,-3)}{4K\rho}$$

$$-\bar{\Theta}\bar{\Pi} \qquad (24)$$

It now remains to evaluate the general integral $I_2(\lambda,y)$.

3.4 The Solution of the General Integral

In order to determine the elements of the velocity distribution it is necessary first to solve the integral given by

$$I_z(\lambda,y) = \int_0^{\infty}\int_0^{2\pi} \exp(-T^2[q+p\cos(2\ell-\phi)])T^{\lambda} \sum_{n=-\infty}^{\infty} J_n(\alpha T) A_z \exp(i\ell(y-n)+i\alpha T\sin\ell)\, d\ell\, dT \tag{1}$$

It will again be convenient to use Bessel functions. The following identities from Watson will be used:

$$\exp[-T^2 p\cos(2\ell-\phi)] = \sum_{k=-\infty}^{\infty} I_k(pT^2)\exp[ik(2\ell-\phi+\pi)] \tag{2}$$

$$\exp[i\alpha T\sin\ell] = \sum_{m=-\infty}^{\infty} J_m(\alpha T)\exp(im\ell) \tag{3}$$

where $I_k(z)$ is the Bessel function of an imaginary argument, defined by

$$I_k(z) = \sum_{n=0}^{\infty} \frac{(z/2)^{k+2n}}{n!(k+n)!} \tag{4}$$

Substituting equations (2) and (3) in equation (1) and rearranging terms, it is found that

$$I_z(\lambda,y) = \int_0^{\infty} T\exp(-qT^2) \sum_{k=-\infty}^{\infty} I_k(pT^2) \sum_{n=-\infty}^{\infty} J_n(\alpha T) A_z \sum_{m=-\infty}^{\infty} J_m(\alpha T) \int_0^{2\pi} \exp[i(k(2\ell-\phi+\pi)+(y-n)\ell+m\ell)]\, d\ell\, dT \tag{5}$$

Clearly, the integral in ℓ will vanish unless

$$y-n+2k+m = 0 \tag{6}$$

If this condition is satisfied, then

$$\int_0^{2\pi} \exp\left[ik(\pi-\phi)\right] d\ell \;=\; 2\pi \exp\left[ik(\pi-\phi)\right] \tag{7}$$

Introducing this into equation (5), the equation becomes

$$I_z(\lambda,y) = \int_0^{\infty} T^{\lambda} \exp(-qT^2) \sum_{k=-\infty}^{\infty} I_k(pT^2) \sum_{n=-\infty}^{\infty} J_n(\alpha T) A_z \sum_{m=-\infty}^{\infty} J_m(\alpha T)\; 2\pi \exp\left[ik(\pi-\phi)\right] dT \tag{8}$$

with the condition that

$$y-n+2k+m = 0 \tag{9}$$

To evaluate equation (8), various properties and relations of the Bessel functions and hypergeometric functions will be used. These can all be found in Watson. The Bessel functions J_n and J_m may be combined by using the relation

$$J_n(x)J_m(x) = \sum_{s=0}^{\infty} (x/2)^{n+m+2s} (-1)^s \frac{(n+m+2s)!}{s!(m+s)!(n+s)!(n+m+s)!} \tag{10}$$

for n and m greater than or equal to zero. When n or m is negative, J_n may be transformed to the corresponding

Bessel function of positive n, J_{-n}, by the identity

$$J_{-n}(x) = (-1)^n J_n(x) \tag{11}$$

Equation (10) can now be generalized to hold for all values of n and m if it is rewritten as

$$J_n(x)J_m(x) = \sum_{s=0}^{\infty} E x^v \tag{12}$$

where $$v = |n| + |m| + 2s \tag{13}$$

$$E = (-1)^s 2^{-v} \left(\frac{n}{|n|}\right)^n \left(\frac{m}{|m|}\right)^m \frac{v!}{s!(|n|+s)!(|m|+s)!(v-s)!} \tag{14}$$

It will be convenient to replace also $I_k(x)$ in equation (8), by using the relation

$$I_k(x) = (-i)^k J_k(ix) \tag{15}$$

With these modifications, equation (8) now becomes

$$I_z(\lambda,y) = \int_0^{\infty} T^{\lambda} \exp(-qT^2) \sum_{n,m,s} E(\alpha T)^v A_z \sum_{k=-\infty}^{\infty} J_k(ipT^2)(-i)^k 2\pi \exp\left[ik(\pi-\phi)\right] dT \tag{16}$$

where

$$\sum_{n,m,s} = \sum_{n=-\infty}^{\infty} \sum_{m=-\infty}^{\infty} \sum_{s=0}^{\infty} \tag{17}$$

The last summation may be reduced with the help of equation (11) by noting that

$$\sum_{k=-\infty}^{\infty} J_k(ipT^2)(-i)^k \exp\left[ik(\pi-\phi)\right] = \sum_{k=1}^{\infty} (i)^k 2\cos k\phi \, J_k(ipT^2) + J_o(ipT^2) \tag{18}$$

If the following change of variables is introduced,

$$x = T^2 \tag{19}$$

then equation (16) is transformed to

$$I_z(\lambda,y) = \pi \sum_{n,m,s} EA_z \alpha^v \int_0^\infty x^w \exp(-qx)\left[\sum_{k=1}^\infty i^k 2\cos k\phi J_k(ipx) + J_o(ipx)\right]dx \tag{20}$$

where

$$w = \frac{v+\lambda-1}{2} \tag{21}$$

Watson has shown that

$$\int_0^\infty \exp(-at) J_n(bt) t^{m-1} dt = {}_2F_1\left(\frac{m+n}{2}, \frac{m+n+1}{2}; n+1; -\frac{b^2}{a^2}\right) \frac{\Gamma(m+n)}{\Gamma(n+1)} a^{-n} \tag{22}$$

where ${}_2F_1$, is the hypergeometric function defined by

$${}_2F_1(a,b;c;z) = \frac{\Gamma(c)}{\Gamma(a)\Gamma(b)} \sum_{n=0}^\infty \frac{\Gamma(a+n)\Gamma(b+n)}{n!\,\Gamma(c+n)} z^n \tag{23}$$

and Γ is the well-known gamma function.

If equation (22) is substituted for the integral in equation (21), it is found that

$$I_z(\lambda,y) = \pi \sum_{n,m,s} EA_z \alpha^v \sum_{k=0}^\infty c_k \cos(k\phi) \Gamma(u_1) {}_2F_1(u_1/2, u_2/2; k+1; p^2 q^{-2}) (-p/2)^k q^{k-w-1} \tag{24}$$

where

$$u_1 = w + k + 1 \tag{25}$$

$$u_2 = w + k + 2 \tag{26}$$

and

$$c_k = \begin{cases} 2 & \text{for } k>0 \\ 1 & \text{for } k=0 \end{cases} \tag{27}$$

From the definition of the hypergeometric function it follows that

$$ {}_2F_1(\ ) = \frac{\Gamma(k+1)}{\Gamma(u_1/2)\Gamma(u_2/2)} \sum_{\ell=0}^{\infty} \frac{\Gamma(u_1/2+\ell)\Gamma(u_2/2+\ell)}{\Gamma(k+\ +1)n!} (p/q)^{2\ell} \tag{28}$$

For the gamma function there exists a duplication formula

$$\Gamma(2z) = (2\pi)^{-\frac{1}{2}}\, 2^{(2z-\frac{1}{2})}\, \Gamma(z)\, \Gamma(z+\tfrac{1}{2}) \tag{29}$$

Applying this twice to equation (28), ${}_2F_1$ is simplified to

$$ {}_2F_1(\ ) = \frac{\Gamma(k+1)}{\Gamma(u_1)} \sum_{\ell=0}^{\infty} \frac{\Gamma(u_1+2\ell)}{\Gamma(k+\ +1)\ell!} (p/q)^{2\ell} \tag{30}$$

If use is made of the fact that for positive integers n

$$\Gamma(n+1) = n! \tag{31}$$

then equation (24) becomes

$$I_z(\lambda,y) = \pi \sum_{n,m,s} EA_z \alpha^{\nu} \sum_{k=0}^{\infty} c_k \cos(k\phi)\ (-2)^{-k} q^{-w-1} \sum_{\ell=0}^{\infty} \frac{(w+k+2\ell)!\,(p/q)^{k+2\ell}}{(k+\ell)!\,\ell!} \tag{32}$$

with the constraint that

$$y-n+2k+m = 0 \tag{33}$$

If equation (33) is rewritten as

$$m = n-y-2k \tag{34}$$

then, on substituting this in equation (32) the summation $\sum_{n,m,s}$ may be replaced by $\sum_{n=-\infty}^{\infty}\sum_{s=0}^{\infty}$. Hence the final form of equation (32) may be written as

$$I_z(\lambda,y) = \pi \sum_{n=-\infty}^{\infty}\sum_{s=0}^{\infty} EA_z\alpha^v \sum_{k=0}^{\infty} c_k \cos(k\phi)\ (-2)^{-k} q^{-w-1} \sum_{\ell=0}^{\infty} \frac{(w+k+2\ell)!}{(k+\ell)!\,\ell!}\ (p/q)^{k+2\ell} \tag{35}$$

Although equation (35) still looks somewhat formidable, the series do in fact converge very rapidly. For this reason it is much more efficient to determine the perturbations in the velocity distribution by this method than by straight numerical integration. If the stars are well-mixed, then p vanishes. The equation then reduces to

$$I_z(\lambda,y) = \pi \sum_{n=-\infty}^{\infty}\sum_{s=0}^{\infty} EA_z\alpha^v w!\, q^{-w-1} \tag{36}$$

3.5 Results

Using the procedure described in the previous sections, it is now possible to determine the distortion due to a spiral density wave on the velocity distribution

of a sub-population of stars. The resulting equations are valid for any arbitrary, unperturbed ellipsoidal velocity distribution and for any degree of exponential or sinusoidal time variation of the spiral pattern.

Thus far, only the linear case has been considered. The non-linear terms can be found by using equation (57) in section 3.1. Since only the first non-linear term is important, the computation is quite straightforward. After the linear term (a_1) has been determined the non-linear term (a_2) can be readily calculated. The elements of the velocity distribution are then found by the same method as used in the linear case. However, since the resulting equations become quite complicated, the develop ment in this thesis will be limited to a discussion of only the linear case.

It is emphasized that the linear approximation is valid only if the perturbation in the distribution function is small compared to the distribution function. This will not be the case when the spiral field is very strong or if the velocity dispersions of the stars are very small. However, Barbanis and Woltjer, using first-order epicyclic theory rather than our method, were able to show that the mean velocities of the stars will be directly proportional to the strength of the spiral field. If this

is so, our estimates for the mean velocities will be valid regardless of the strength of the field or the size of the velocity dispersion.

In considering perturbations in the velocity dispersions we will be interested only in the spiral pattern now existing. The linear approximation gives reliable results if the velocity dispersion is greater than about 20 km/sec. The use of the linear approximation is, therefore, justified in such cases.

The parameters of the spiral pattern were taken to be those used by Lin, Yuan and Shu. They are listed in Table XIII. Yuan (1969 I,II) has shown that the parameters must be limited to quite narrow ranges. Hence the values in Table XIII must be near to the actual ones. If the reference position is (8.26 kiloparsec, 0°), then the center of the nearest spiral arm at the same galacto-centric distance as the Sun will be situated $70^{\circ}.5$ clockwise from the Sun.

Our method was checked by comparing our results with those obtained using Lin's approach. This could, of course, be done only for the case where the stars were well-mixed and the pattern was not time dependent. From Table XIV it can be seen that the agreement is good, as should be the case. The small differences are caused by

the fact that we have determined the mean velocities to an accuracy of 3%, this being sufficiently accurate for our purposes.

To determine the sensitivity of the perturbed velocity distribution to the choice of initial axis ratio and vertex deviation, the components of the perturbed velocity distribution were calculated for various values of the axis ratio and vertex deviation. The results are summarized in Tables XV to XX. The velocity dispersions and axis ratios in each table refer to the unperturbed values. It is readily seen that the perturbed velocity distribution is highly sensitive to the values of the unperturbed axis ratio and vertex deviation. In all cases, the components are most sensitive to the unperturbed distribution at low velocity dispersions. As the dispersion increases, the sensitivity declines.

CHAPTER 4

COLLISIONLESS RELAXATION IN THE GALAXY

4.1 Introduction

In the previous chapter it has been shown that the response of a sub-population of stars to a perturbation in the galactic gravitational field depends to a large extent on the parameters of the unperturbed velocity distribution. The time-variation of the distribution parameters will now be examined.

When stars are formed, their velocity distribution is primarily determined by the internal and systematic motions of the parent gas clouds. However, due to the fact that stars with differing velocities will have differing periods, the stellar orbits will gradually get out of step with each other. Such orbital mixing causes the initial conditions to be smoothed out. The approach to a well-mixed state will be referred to as "relaxation", while the well-mixed state itself will be described also by the term "equilibrium". By this is meant a dynamic, rather than a statistical, equilibrium.

The relaxation of stellar sub-populations with various initial conditions will be examined. This will

be done by calculating the orbits of the individual stars by means of first-order epicycle theory. The parameters of the velocity distribution will then be determined for various values of time by integrating over all the orbits at a particular location in the Galaxy.

4.2 The Epicycle Theory

Although the epicyclic theory has been described in detail by Mihalas (1968), Chandrasekhar (1942) and others, a brief account will be given here. Motion only in the galactic plane will be considered.

Consider a star initially with co-ordinates (R_o, θ_o) having a tangential velocity Θ, equal to the circular velocity $\Theta_c(R_o)$ but with a small radial velocity Π_o. The orbit of the star will now be considered using a rotating co-ordinate system centered at R_o and moving with velocity Θ_o about the galactic center.

If r is the distance to the center of the Galaxy and if U(r) is the gravitational potential of the Galaxy, then the radial acceleration of the star is given by

$$\ddot{r} = -\frac{\partial U}{\partial r} + r\dot{\theta}^2 \qquad (1)$$

Since at any arbitrary point

$$\Theta = r\dot{\theta} \qquad (2)$$

and

$$\frac{\partial U}{\partial r} = -\frac{\Theta_c^2}{r} \tag{3}$$

equation (1) may be rewritten as

$$\ddot{r} = \frac{\Theta^2}{r} - \frac{\Theta_c^2}{r} \tag{4}$$

If we now write

$$r = R_o + x \tag{5}$$

where x is the change in r due to the radial velocity Π , then

$$\ddot{r} = \ddot{x} \tag{6}$$

Due to conservation of angular momentum

$$\Theta r = \Theta_o R_o \tag{7}$$

Hence

$$\frac{\Theta^2}{r} = \frac{\Theta_o^2 R_o^2}{r^3} \tag{8}$$

If we assume x is small compared to r then, on substituting for r and carrying only first-order terms, we find

$$\frac{\Theta^2}{r} = \left(\frac{\Theta_o^2}{R_o}\right)\left(1-\frac{3x}{R_o}\right) \tag{9}$$

If x is small the circular velocity Θ_c may be expanded in the solar neighbourhood by a Taylor's series. To first-order, we obtain

$$\Theta_c(r) = \Theta_c(R_o) + \left(\frac{\partial \Theta_c}{\partial r}\right)_{R_o} x \qquad (10)$$

Squaring equation (10) and dividing by r, we find to first-order that

$$\frac{\Theta_c^2(r)}{r} = \frac{\Theta_o^2}{R_o} + 2\left(\frac{\partial \Theta_c}{\partial r}\right)_{R_o} \frac{\Theta_o x}{R_o} - \frac{\Theta_o^2 x}{R_o^2} \qquad (11)$$

On substituting equations (6), (9) and (11) in equation (4), the equation may be reduced to

$$\ddot{x} = -K^2 x \qquad (12)$$

where K is called the "epicyclic frequency" and is defined by

$$K = \left(\frac{2\Theta_o^2}{R_o^2} + 2\left(\frac{\partial \Theta}{\partial r}\right)_{R_o} \frac{\Theta_o}{R_o}\right)^{\frac{1}{2}}$$

A solution to equation (12) is

$$x = \frac{\Pi_o}{k} \sin kt \qquad (13)$$

$$\dot{x} = \Pi = \Pi_o \cos kt \qquad (14)$$

Hence, knowing the initial radial velocity Π_o, it is possible to determine the galactocentric distance $(R_o + x)$ and the radial velocity Π at any later time.

Using similar approaches, the tangential velocity can also be found. Since angular momentum is conserved, it follows that

$$\dot{\theta} = \frac{R_o \Theta_o}{r^2} = \left(\frac{\Theta_o}{R_o}\right)\left(1 - \frac{2x}{R_o}\right) \qquad (15)$$

Again, we have neglected second-order terms. The difference in the angular velocity between the star and the epicyclic frame is

$$\Delta\dot{\theta} = -\frac{2\times\Theta_o}{R_o^2} \qquad (16)$$

Substituting equation (13) and converting to a linear velocity, this becomes

$$\Delta\Theta = \Delta r\dot{\theta} = -2\left(\frac{\Pi_o\Theta_o}{kR_o}\right)\sin Kt \qquad (17)$$

In determing the mean peculiar velocity of a group of stars which are at a certain position (r,θ) and which have differing initial conditions and orbital parameters, we are not interested in the mean $\Delta\Theta$ but in the mean of $(\Theta(r) - \Theta_c(r))$. To first-order, this is found to be given by

$$\Theta(r) - \Theta_c(r) = -\left(\frac{R_o\Pi_o K}{2\Theta_o}\right)\sin Kt \qquad (18)$$

Since equations (14) and (18) provide a very simple first-order estimate of the peculiar velocity components of a star at any time they will be very useful in this chapter. The main limitation of the epicycle theory comes from the fact that only first-order terms have been carried. Although this causes some discrepancies between the actual and estimated orbits when the epicyclic amplitude is large, the differences are very small for stars with small peculiar velocities.

4.3 Mathematical Formulation

The general case will be considered where a sub-population of stars initially has mean velocity components u and v in the radial and transverse directions, respectively. The initial velocity distribution about the mean velocities need not be at equilibrium but is assumed to be of the form

$$f = c \exp(-x_o \Pi^2 - y_o \Theta^2 - 2z_o \Theta\Pi) \qquad (1)$$

where c is a constant, Π and Θ are the radial and transverse velocity components with respect to the mean velocity and x_o, y_o and z_o are defined as follows:

$$x_o = \frac{\sigma_\Theta^2}{2(\sigma_\Theta^2\sigma_\Pi^2 - \sigma_{\Theta\Pi}^4)} \qquad (2)$$

$$y_o = \frac{x_o\sigma_\Pi^2}{\sigma_\Theta^2} \qquad (3)$$

$$z_o = -\frac{x_o\sigma_{\Theta\Pi}^2}{\sigma_\Theta^2} \qquad (4)$$

The velocity dispersions, the mean velocity components and the constant c may vary with the spatial coordinates.

Consider a star initially at (R_o, θ_o) with an initial velocity (with respect to the mean velocity) of (Π_o, Θ_o). The total peculiar velocity (Π_o', Θ_o') is then given by (Π_o+u, Θ_o+v) and the probability of finding such

a star is $f(\theta_o, R_o, \Pi_o, \Theta_o)$. The distance R_o is related to the galacto-centric distance of the epicyclic frame, R_1, by

$$R_o = R_1 + \frac{a(\Theta_o + v)}{k} \tag{5}$$

where, if Ω denotes the angular velocity of the epicyclic frame, a is defined as

$$a = \frac{2\Omega}{k}$$

At a time t later, the probability of such a star existing will, of course, still be the same. Its position and velocity will, however, have changed as follows:

$$\Pi' = (\Pi_o + u)\cos kt + a(\Theta_o + v)\sin kt \tag{6}$$

$$\Theta' = (\Theta_o + v)\cos kt - \frac{1}{a}(\Pi_o + u)\sin kt \tag{7}$$

$$R' = R_1 + a\Theta' \tag{8}$$

$$\theta' = \theta_o + \Omega t + \frac{a}{k}(\Pi' - \Pi_o - u) \tag{9}$$

If the perturbations are such that the variations of the parameters with θ are slow compared to the variations with R, as in the case of spiral waves with small angles of inclination, then θ' may be approximated to first order as

$$\theta' = \theta_o + \Omega t \tag{10}$$

We now define

$$\Pi = \Pi_o \cos kt + a \sin kt \qquad (11)$$

$$\Theta = \Theta_o \cos kt - \frac{\Pi_o}{a} \sin kt \qquad (12)$$

These correspond to the velocity components the star would have had if initially no mean velocity (u, v) existed. In terms of Π and Θ, equations (6) to (7) become

$$\Pi' = \Pi + u \cos kt + av \sin kt \qquad (13)$$

$$\Theta' = \Theta + v \cos kt - \frac{u}{a} \sin kt \qquad (14)$$

$$R' = R_1 + \frac{a}{k} (\Theta + v \cos kt - \frac{u}{a} \sin kt) \qquad (15)$$

The probability of finding the star may also be written in terms of Π and Θ, as

$$f = f(\theta' - \Omega t,\ R' - a(\Theta + v\cos kt - \frac{u}{a}\sin kt), \Pi \cos kt - a\Theta \sin kt, \Theta \cos kt + \frac{\Pi}{a}\sin kt) \qquad (16)$$

This may be rewritten more conveniently as

$$f = c \exp (-x\Pi^2 - y\Theta^2 - 2z\Theta\Pi) \qquad (16a)$$

where

$$x = \tfrac{1}{2}(x_o - \frac{y_o}{a^2})\cos 2Kt + \tfrac{1}{2}(x_o + \frac{y_o}{a^2}) - \frac{z_o}{a} \sin 2Kt \qquad (17)$$

$$y = \tfrac{1}{2}(y_o - \frac{x_o}{a^2})\cos 2Kt + \tfrac{1}{2}(y_o + \frac{x_o}{a^2}) + z_o a \sin 2Kt \qquad (18)$$

$$z = \tfrac{1}{2}(\frac{y_o}{a} - ax_o)\sin 2Kt + z_o \cos 2Kt \qquad (19)$$

To determine the components of the velocity distribution it is necessary to find the averages of all the individual stellar velocity components weighted by their respective probabilities. From equation (16) it is evident that the probability of finding a star with the velocity (Π, Θ) is dependent on time. In the case of a well-mixed initial distribution the time-dependent terms vanish, as would be expected. The stars will be averaged at a particular position (R', θ'). Since the quantities R' and θ' may therefore be considered to be known, it remains to find θ_o, R_o, k and Ω for each value of (Π, Θ).

If Maarten Schmidt's (1965) mass model of the Galaxy is used, the angular velocity Ω and the epicyclic frequency K can be determined for various values of R_1. To simplify the determination of the relationships, polynomials were fitted through the values of Ω and k by using a least squares fit. The best fits were found to be given by the following polynomials.

$$\Omega(R) = 72.559 - 6.5874R + 0.18254R^2 \qquad (20)$$

$$K(R) = 140.55 - 15.906R + 0.50856R^2 \qquad (21)$$

A comparison between the values from equations (21) and (22) and those derived directly from Schmidt's model is shown in Table XXI.

The initial distance R_o is related to the distance R' at time t by

$$R_o = R' + \frac{a}{k}(\Theta - v)(\cos kt - 1) + \frac{u+\Pi}{k}\sin kt \qquad (22)$$

If u and v depend on R_o while Ω and K depend on R_1, the solution for R_o and R_1 is non-trivial. However, if we consider the ratio of the spiral force to the total galactic gravitational force to be of the same order as the ratio of the epicyclic amplitude to R_1, the variation of u and v over the epicylic orbit is of second order and can thus be neglected. The value of R_1 may then be found by substituting equations (20) and (21) into equation (15) and iterating. Knowing R_1, it is now possible to calculate k, Ω and θ_o.

The components of the velocity distribution at (R', θ') may be found by integrating the individual velocity components and combinations thereof over all values of (Π, Θ). Since R_1 (and hence k, Ω and θ_o) are independent of Π, integration over Π is trivial. Using equation (16a), the following integrals were evaluated:

$$\int_{-\infty}^{\infty} \Pi f d\Pi = -\frac{cZ}{x}\left(\frac{\pi}{x}\right)^{\frac{1}{2}} \exp\left(\left(\frac{Z^2}{x} - y\right)\Theta^2\right) \qquad (23)$$

$$\int_{-\infty}^{\infty} f d\Pi = c\left(\frac{\pi}{x}\right)^{\frac{1}{2}} \exp\left(\left(\frac{Z^2}{x} - y\right)\Theta^2\right) \qquad (24)$$

$$\int_{-\infty}^{\infty} \Pi^2 f d\Pi = \frac{c}{2x}\left(1 + \frac{2Z^2}{x}\Theta^2\right)\left(\frac{\pi}{x}\right)^{\frac{1}{2}} \exp\left(\left(\frac{Z^2}{x} - y\right)\Theta^2\right) \qquad (25)$$

Since K, Ω and θ_o all depend on Θ, integration over Θ is, unfortunately, not so trivial. Numerical integration techniques must be applied. The UBC Library Subprogram COSIM was used. This program integrates functions by means of a stratified form of Romberg integration which uses Simpson's rule on strips of varying widths.

The components of the velocity distribution were then found to be

$$\bar{\Pi}' = H\left(-\frac{Z}{x}\Theta + u\cos kt + av\sin kt\right) \qquad (26)$$

$$\bar{\Theta}' = H\left(\Theta + v\cos kt - \frac{u}{a}\sin kt\right) \qquad (27)$$

$$\sigma_{\Pi}^2 = H\left(\frac{x}{2}\left[1 + \frac{2Z^2\Theta^2}{x}\right] - 2\frac{Z}{x}\Theta\left[u\cos kt + av\sin kt\right] + u^2\cos^2 kt + a^2v^2\sin^2 kt + auv\sin 2kt\right) - \bar{\Pi}'^2 \qquad (28)$$

$$\sigma_{\Theta}^2 = H\left(\Theta^2 + 2\Theta\left[v\cos kt - \frac{u}{a}\sin kt\right] + v^2\cos^2 kt + \frac{u^2}{a^2}\sin^2 kt - \frac{uv}{a}\sin 2kt\right) - \bar{\Theta}'^2 \qquad (29)$$

$$\sigma_{\Theta\Pi}^2 = H\left(-\frac{Z}{x}\Theta^2 + \Theta\left[u\cos kt + av\sin kt - \frac{Z}{x}v\cos kt + \frac{Zu}{xa}\sin kt\right] + uv\cos 2kt + \left[av^2 - \frac{u^2}{a}\right]\frac{\sin 2kt}{2}\right) - \bar{\Theta}'\bar{\Pi}' \qquad (30)$$

where

$$H(x) = \frac{\int_{-\infty}^{\infty} x \exp\left[\left(\frac{Z^2}{x} - y\right)\Theta^2\right] d\Theta}{\int_{-\infty}^{\infty} \exp\left[\left(\frac{Z^2}{x} - y\right)\Theta^2\right] d\Theta} \qquad (31)$$

4.4 Results

The relaxation of a number of sub-populations having various initial velocity distributions was examined. In each case, equilibrium was approached after a time in the order of 10^9 years. Two of the cases are discussed below in more detail.

In the first case it was assumed that the sub-population was at equilibrium and that all the stars then instantaneously received a velocity increment u of 10 km/sec. The initial velocity dispersion was 20 km/sec. The variation of the velocity components with time is shown in Figures 5 to 9. The mean velocities oscillate with a period of 2×10^8 years which corresponds to the epicyclic period. However, due to orbital mixing, the oscillations are gradually damped. At 4×10^8 years they have decayed to half their original amplitudes. They have all but vanished after 10^9 years. The velocity dispersion oscillates with a period of 10^8 years but increases steadily. It is important to note that the vertex deviation and the axis ratio also experience oscillations. After 10^9 years all oscillations have ceased, the stars have again reached equilibrium and the only change has been an increase in the velocity dispersion. For this case, the amplitudes of the oscillations are, in general, governed by the choice of u and v. The time for equilibrium to be reached (i.e.

for mixing to be completed) depends solely on the initial velocity dispersions. Here it was assumed, for simplicity, that u did not vary with θ_o. If u does depend on θ_o, the same equations can still be used but more parameters are needed to specify the dependence of u on θ. For spiral arms with low inclinations, this will make little difference in the results. It was also assumed that c was independent of θ and R.

In the second case under consideration, it was assumed that no mean velocities existed, but that the radial velocity dispersion equalled the transverse velocity dispersion. It was again assumed that the effect was axi-symmetric. Results are shown in Figures 10 to 14 for an initial dispersion of 17 km/sec. The resulting curves show features similar to those discussed in the first case. Equilibrium is again reached after a time of about 10^9 years and an increase in the velocity dispersion is obtained.

From these studies it can be concluded that a sub-population of stars will approach equilibrium even in the absence of collisions. The relaxation time for the system depends entirely on the initial velocity distribution. It has been shown that the collisionless relaxation is accompanied by an increase in the velocity dispersion and also that, for sub-populations not at equilibrium, the

mean velocities and the vertex deviation are in general non-vanishing. It should be noted that the collisionless relaxation does not depend on the masses of the individual stars.

The phenomenon of orbital mixing has also been discussed by Lynden-Bell (1962), among others. His treatment was, however, limited to a qualitative description and did not include an examination of the time variation of the velocity distribution parameters.

CHAPTER 5

THE VERTEX DEVIATION

A relationship between the vertex deviation and the velocity dispersion has been found in Chapter 1 (see Table II). The results have been plotted in Figure 15. The crosses refer to our data points while the triangles represent Delhaye's weighted mean values for various sub-populations. As can be seen, there is a good agreement. The dashed line represents the expected relationship for well-mixed stars perturbed by the present spiral density pattern. It is apparent that the estimates from the wave theory are significantly lower than the observational values. If the observations are considered to be reliable, it follows that some assumption in the theoretical approach must be invalid.

The gravitational field has been assumed to be completely represented by a two-armed spiral density wave superimposed upon the axi-symmetric gravitational field. It is, however, a well-known observational fact that local irregularities in the spiral arms do occur. The Sun is located in such an irregularity, the inter-arm Orion spur. According to Yuan (1971), the presence of the Orion spur

may cause a deviation of the vertex of the relatively old stars but the velocity distribution of the younger stars is unlikely to be influenced by it. Since the nature of the effect is at present not well understood from either the observational or theoretical point of view, it is, unfortunately, impossible to determine a reasonable estimate of any vertex deviation it may cause. It appears to be possible, at any rate, that the presence of the Orion spur may explain the observed vertex deviation of the older stars.

Such an explanation will not suffice for the young stars. However, it has been assumed that the stars are well-mixed. Since it was shown in the previous chapter that about 10^9 years are required before mixing can be completed, it is expected that populations younger than this will still have retained some memory of their origin. From Table X it appears likely that the first three age groups are not yet well-mixed. This brings us to a maximum velocity dispersion of 21 km/sec for group 3. It must therefore be considered that, in determining the response of stars to the spiral field, the younger groups (with small velocity dispersions) are not yet well-mixed.

According to Roberts (1970), stars are formed in the spiral arms. The velocity dispersion of the newly born stars will be due primarily to the turbulent velocity

of the parent gas cloud. Velocities are also imparted to the gas balls, out of which the stars are formed, by heat and radiation pressure emitted from recently formed O-stars. Since these effects are unrelated to the galactic rotation, the initial velocity dispersion will be isotropic (i.e. the radial and transverse velocity dispersions will be equal).

The youngest stars were found to have a velocity dispersion of about 15 km/sec. If this is corrected for the effect due to the spiral arm, it corresponds to an unperturbed velocity dispersion of about 17 km/sec (see Table XVIII). It is assumed that this is the value of the initial velocity dispersion. At formation, the mean velocity of the stars will equal that of the parent gas complex. Since, in general, this will be smaller in magnitude than the mean velocity which the spiral wave will impart to the stars, no mixing will occur as a result of the initial mean velocity.

After formation, the isotropic velocity distribution will cause orbital mixing. Simultaneously, the presence of the spiral waves will influence the stellar motions. These effects may be separated if the amplitude of the spiral pattern does not change significantly during the mixing process. If the amplitude decreases then additional mixing will occur due to the resulting decrease in the mean velocity imparted by the spiral waves. This

complicates the analysis considerably. For convenience, it will be assumed here that the amplitude is independent of time. In the next chapter, where the time-dependence of the spiral pattern will be estimated, the validity of this assumption will be checked.

The time-dependence of the velocity distribution was determined in the following manner. The stars were considered to be formed near the centres of the spiral arms. Orbital mixing was then assumed to occur. This was entirely due to the initial isotropic velocity distribution which had a value of 17 km/sec. Neglecting the influence of the spiral arms, the components of the velocity distribution were found for various times by the method described in the previous chapter. These were then corrected for the effect of the spiral arms.

If the Sun is located $70^{\circ}.5$ counterclockwise from the center of the nearest spiral arm at the same distance from the galactic center and if the pattern has an angular velocity of 13,5 km/sec/kpc, then the time required for stars to migrate from the spiral arm to the Sun is 1.6×10^8 years. Stars from the other arm arrive after 4.2×10^8 years. The velocity dispersions and vertex deviations corresponding to these times are represented by the dots in Figure 15. They appear to agree quite well with the observed relation.

Since the initial distribution function varied with the spatial co-ordinates, it was implicitly assumed that the velocity distribution had not changed appreciably due to the mixing of the original group of stars with neighbouring stars. On examining this assumption in detail, it was found that after 4.2×10^8 years the distribution parameters had changed, through spatial mixing, by no more than 10 per cent. The approximation is thus justified for times less than 4.2×10^8 years.

It is concluded that the large deviation of the vertex which has been observed for the young stars may be explained by the fact that the orbital mixing of these stars has not yet been completed. When this effect is combined with that of the spiral arms the resulting relationship between the velocity dispersion and the vertex deviation agrees well with the observational result.

CHAPTER 6

THE AGE DEPENDENCE OF THE VELOCITY DISTRIBUTION

6.1 Introduction

The orbital mixing of initial conditions which was shown to cause an increase in the velocity dispersion of young stars cannot explain the large dispersions observed for older stars. Although the presence of a spiral density wave causes variations in the velocity distribution of a stellar sub-population, no net change is recorded when these are averaged over all angles. Thus far it has been assumed that the wave amplitudes do not vary with time. However, Toomre (1969) has found that unless the waves are somehow replenished, interactions between the stars and the waves will cause the waves to be damped. The effect of such decaying waves on the stellar velocity dispersion will now be examined.

The following first-order model is proposed. Spiral waves are initially caused by some unknown mechanism far from the local vicinity. As the waves propagate over the galactic disk energy is transferred from the source. It is assumed that while the wave is growing the stellar velocity dispersion increases by a negligible amount. This implies that the growth must be rapid ($\ll 10^9$ years). In the model of Marochnik and Suchkov only a few times 10^8 years are

needed for spiral waves to form. A similar timescale is found by Toomre (1969) if the spiral waves are due to a close encounter with the Large Magellanic Cloud. The assumption of rapid growth hence seems reasonable.

Since Pomagaev finds that the perturbations of the stellar velocity distribution are determined primarily by the gravitational field when the waves have completed their growth, the assumption of rapid growth will not effect the final perturbations.

According to Toomre (1969), non-linear effects become important when the rapid growth is completed. Interactions between the stars and the waves cause the waves to be damped. This stems from a slight phase mixing of the perturbed oscillations of various stars even in the presence of those collective forces that maintain the spiral wave. As the waves decay the velocity dispersions of the stars will increase by an amount equal to the loss of gravitational energy of the wave. Since the damping is of a Landau nature it is assumed (as suggested by Harrison) that the time variation be exponential.

If we were interested in the time-dependence of the velocity distribution of a particular sub-population, then orbital and spatial mixing would have to be taken into account. However, since all the observations were taken at the present epoch, no memory of mixing will have remained except for the velocity increments obtained within the last 10^9 years. Mixing may thus be assumed to have been completed for stars older than 10^9 years if the most recent increments are neglected. The effect of orbital mixing may then be considered to occur instantaneously and the orbits may be averaged over all angles.

It is assumed that, as the spiral wave decays, the excess mean velocity of the gas in the galactic disk is lost very rapidly due to collisions among the clouds. The mean velocity of the gas will therefore be considered to be that due to the spiral field. It is assumed also that the turbulent velocity of the gas does not change appreciably, so that all stars will have the same velocity dispersion at formation.

6.2 Mathematical Formulation

The amplitudes of the mean motions and the density fluctuation due to the spiral field will be denoted by u_1, v_1 and ρ_1, respectively. At a time t the mean motions and the density may be written as

$$\rho(t) = \rho_o(1 + \rho_1 \exp(i\psi + \beta t)) \quad (1)$$

$$u(t) = \frac{u_{1\,o} \exp(i\psi + \beta t)}{\rho} \quad (2)$$

$$v(t) = \frac{u(t) v_1}{u_1} \quad (3)$$

where ρ_o is the average density, β represents the decay rate and ψ is the angular position with respect to the spiral arms.

Averages will now be taken over all angles ψ. Since the variation in star density with ψ suggests that stars spend more time in the denser regions, the chances that a star will obtain an orbital velocity increment there are correspondingly greater. A weighting term $\frac{\rho}{\rho_o}$ should therefore be applied. It is then found that the average density equals the unperturbed value and the average velocities vanish.

It is assumed that as the wave decays the loss of gravitational energy of the wave is accompanied by an increase in the energy of peculiar motions. This is

equivalent to assuming that the mean velocities of the stars due to the spiral wave will be converted to a corresponding increase in the stellar velocity dispersions.

After averaging over all angles ψ it is found that

$$u^2(t) = \tfrac{1}{2}u_1^2 \exp(2\beta t) \qquad (4)$$

$$v^2(t) = \tfrac{1}{2}v_1^2 \exp(2\beta t) \qquad (5)$$

For stars which had been formed before the decay began, the resulting changes in the oscillation amplitudes will correspond to an increase in the velocity dispersions of

$$\Delta\sigma_u^2 = \tfrac{1}{4}(u_1^2 + 2.5v_1^2)(1 - \exp(2\beta t)) \qquad (6)$$

for stars near the Sun. For stars which were formed at a time t_o after the beginning of the decay, this becomes

$$\Delta\sigma_u^2 = \tfrac{1}{4}(u_1^2 + 2.5v_1^2)(\exp(2\beta t_o) - \exp(2\beta t)) \qquad (7)$$

These equations will be used to determine the theoretical relation between age and velocity dispersion.

6.3 Results

Since for young stars mixing has not yet been completed, only stars older than 10^9 years were used in determining the age-dependence of the velocity dispersion.

The quantities in Table XI were corrected (for the effect of the present spiral wave) to the unperturbed values. The velocity dispersions were squared and plotted in Figure 16.

At first sight it might appear that the large velocity dispersions of the older stars could be explained if these stars had been formed during the initial collapse of the early Galaxy to its present form. However, according to Eggen, Lynden-Bell and Sandage (1962) the collapse was very rapid, lasting only about 10^8 years. Stars formed during this time would be expected to exhibit very large velocities perpendicular to the galactic plane. Since no such velocities are apparent, it follows that these stars have most likely been formed after the initial collapse.

From Figure 16 it is evident that the square of the dispersion increases from 400 to 3000 km^2/sec^2 in 11×10^9 years. The possibility of such an increase being due to just one spiral pattern will now be investigated. If A denotes the amplitude of the present spiral field, β represents the decay rate and A_o is the maximum amplitude of the spiral field 12×10^9 years ago, then

$$A = A_o \exp(-12\beta \times 10^9) \qquad (1)$$

Stars initially having an isotropic velocity dispersion of 17 km/sec will soon become mixed, causing the radial velocity dispersion to reach 22 km/sec. A spiral field of the present strength (5 per cent of the mean gravitational field) will cause a mean velocity (u, v) of an amplitude of about (7, 1) km/sec. When the spiral field has vanished, this will correspond to an increase in the square of the radial velocity dispersion of 13 km^2/sec^2. The difference in the square of the dispersion between the youngest and oldest stars is then given by

$$\Delta\sigma_u^2 = 2600 = \frac{13(A_o^2-1)}{A^2} \qquad (2)$$

Solving equations (1) and (2), it is easily found that the initial amplitude of the wave must have been 14 times the present amplitude. The reciprocal of β is then 4.4×10^9 years. When the age-dispersion relation corresponding to such a pattern (curve a) is compared to the observational curve in Figure 16 it is evident that large discrepancies exist between the two. It was thus concluded that more than one pattern must have existed.

It was found that if two spiral patterns have existed the resulting curve (curve b in Figure 16) coincided quite nicely with the observations. The maximum amplitudes of the waves were 6 and 14 times the present

pattern amplitude. The β reciprocals were found to be 1.3×10^9 and 3.0×10^9 years, respectively. In determining the theoretical curve it should be taken into consideration that the mean velocity caused by the spiral wave is dependent on the velocity dispersion of the stars. This is important only for the older stars whose velocity dispersions have been significantly increased by the first spiral wave. Since the uncertainties involved are large, it is, of course, possible to fit various combinations of patterns to the curve. However, the break in the curve at 2.4×10^9 years and the rapid increase at 10^{10} years do suggest that at least two major patterns have existed.

The break at 2.4×10^9 years was examined closely to ensure that it is real and not due to uncertainties in the stellar ages. After eliminating the main sequence stars and others having large age uncertainties, it was found that the break still existed, becoming perhaps even more distinct. It was therefore concluded that the break was not a result of uncertainties in the ages. Figure 17 shows that the same spiral patterns can be fitted to the revised curve.

In the preceding chapter it was assumed that the amplitude of the spiral wave had not changed appreciably during the mixing process. If the present pattern is the residue of a spiral wave 6 times the amplitude of

the present wave and if the decay started 2.4×10^9 years ago, then the amplitude of the wave 4.2×10^8 years ago would have been 1.28 times the present amplitude. Such changes are small enough to be neglected.

The decay was assumed to be exponential. If, however, the decay were more rapid than assumed then it follows that the present wave could not be a remnant of the wave whose decay began 2.4×10^9 years ago. At least three spiral waves are then needed to explain the observations.

It was also assumed that all the wave energy is eventually transformed into an increase in the velocity dispersions of the stars. If, in fact, only a fraction of the wave energy is thus transferred (as suggested by Toomre) then the wave amplitudes must be increased correspondingly to account for the observed effect.

The uncertainties in the observational curve and in the assumptions regarding the stellar velocity dispersions at star formation and the growth and decay of spiral waves suggest that not too much emphasis should be put on the actual numerical values here obtained. What is important is that the proposed model can be used to explain the observed age effect rather simply. It is hoped that in the future new, more accurate data and a deeper understanding of the origin and evolution of spiral waves will permit a more precise determination of the history of spiral patterns in our Galaxy.

CHAPTER 7

CONCLUSION

From the evolutionary tracks of stellar models it was possible to estimate ages for a number of stars. The age dependence of the velocity distribution of the nearby stars could then be found. A relationship was also found between the velocity dispersion and the vertex deviation.

The phenomenon of collisionless relaxation due to a non-equilibrium initial velocity distribution was investigated. The sub-population of stars soon approached dynamic equilibrium as a result of orbital mixing.

A method for determining the response of a non-equilibrium sub-population to a spiral density wave was developed. The response was found to be quite sensitive to the form of the velocity distribution.

It was found that the deviation of the vertex for young stars could be caused by the effect of the present spiral wave on a sub-population of stars whose orbital mixing has not yet been completed. For the older stars,

the vertex deviation may be due to the presence of the Orion spur.

The increase of the velocity dispersion with age was explained by postulating that the spiral pattern has decayed and reformed a number of times. A good agreement with observation was obtained if two spiral patterns have existed with amplitudes of 6 and 14 times the present amplitude and with decay rates of 1.3×10^9 and 3×10^9 years, respectively.

TABLES

TABLE I

Variation of Velocity Distribution with Spectral Type

Spectral Type	Number	Mean Velocities (km/sec) u	v	w	Velocity Dispersions (km/sec) σ_u	σ_v	σ_w	Vertex Deviation
B5-A9	30	- 3.0	- 6.6	- 7.3	16.5	8.4	5.1	17°.3
F0-F4	41	-17.1	-10.4	- 6.9	20.8	15.3	12.8	22°.2
F5-F9	96	-10.7	-13.0	- 8.3	26.5	17.0	15.0	8°.4
G0-G4	118	-17.2	-21.4	- 4.3	36.4	24.6	20.8	12°.9
G5-G9	103	- 9.2	-25.2	-10.1	34.4	29.3	17.3	23°.9
K0-K4	167	-12.6	-19.7	- 7.5	35.6	23.1	18.6	14°.3
K5-K9	157	-11.1	-23.3	- 7.7	35.0	21.4	18.8	14°.0
M0-M9	321	- 6.8	-21.4	- 8.5	40.8	49.6	20.7	-12°.0
sub dwarf	21	-10.4	-31.1	4.2	63.2	71.4	43.3	-38°.2
white dwarf	23	18.8	-82.1	- 3.4	112.5	119.9	39.1	42°.4

TABLE II

Adjusted Velocity Distributions

Spectral Type	Number	Mean Velocities (km/sec)			Velocity Dispersions (km/sec)			Vertex Deviation (°)	Axis Ratio
		u	v	w	σ_u	σ_v	σ_w		
B5-A9	30	- 3.0	- 6.6	- 7.3	16.5	8.4	5.1	17.3	0.26
F0-F4	39	-16.7	- 8.8	- 6.9	20.1	13.2	13.1	22.7	0.44
F5-F9	89	-11.0	-13.9	- 7.8	24.2	13.9	15.0	13.2	0.33
G0-G4	95	-12.9	-14.5	- 3.8	26.2	17.2	17.5	15.2	0.43
G5-G9	93	- 7.9	-18.8	- 9.4	26.3	19.6	15.6	15.6	0.55
K0-K4	154	-12.6	-17.7	- 7.1	31.4	19.1	18.1	8.2	0.37
K5-K9	140	- 8.4	-20.0	- 6.6	30.7	18.3	16.7	5.3	0.36
M0-M9	291	- 7.2	-15.5	- 9.0	31.4	19.3	18.8	5.7	0.38
white dwarfs	22	- 2.0	-16.5	- 3.3	49.9	26.0	42.4	-8.8	0.27
sub-dwarfs	18	-18.8	-34.8	-19.4	56.0	33.4	31.2	0.7	0.36

TABLE III

Velocity Distributions from Medians

Spectral Type	Number	Median Velocities (km/sec) u	v	w	Velocity Dispersions (km/sec) (from medians) σ_u	σ_v	σ_w	Axis Ratios
B5-A9	30	- 4	- 8	- 9	17.8	8.9	4.5	0.25
F0-F4	39	-15	-11	-10	20.8	13.4	11.9	0.42
F5-F9	89	- 9	-16	- 9	28.2	13.4	10.4	0.23
G0-G4	95	-18	-15	- 4	25.2	19.3	14.8	0.59
G5-G9	93	- 6	-18	- 9	26.7	19.3	10.4	0.52
K0-K4	154	-15	-16	- 8	31.1	14.8	14.8	0.23
K5-K9	140	-11	-19	- 8	26.7	14.8	14.8	0.31
M0-M9	291	- 9	-14	-10	35.6	16.3	14.8	0.21
white dwarfs	22	- 2	-15	- 4	59.3	14.8	32.6	0.06
sub-dwarfs	18	-18	-33	-21	56.4	38.6	13.4	0.47

TABLE IV

The Zero-Age Main Sequence from Schlesinger's Formulae

M	log L	M_b	M_v	(B-V)	t_1 (10^9 yrs)	t_2 (10^9 yrs)
1.0	0.0	4.72			3.8	3.0
1.1	0.062	4.565	4.64	0.57	2.6	2.1
1.2	0.250	4.095	4.16	0.49	1.9	1.45
1.3	0.419	3.67	3.73	0.43	1.45	1.08
1.4	0.572	3.29	3.35	0.37	1.13	0.83
1.5	0.712	2.94	3.01	0.31	0.92	0.65
1.6	0.841	2.62	2.695	0.25	0.75	0.52
1.7	0.960	2.32	2.41	0.18	0.62	0.42
1.8	1.071	2.04	2.16	0.13	0.53	0.35
1.9	1.175	1.78	1.95	0.08	0.45	0.30
2.0	1.272	1.54	1.75	0.04	0.39	0.25
2.1	1.363	1.31	1.59	0.01	0.34	0.215
2.2	1.449	1.08	1.42	-0.005	0.30	0.19
2.3	1.531	0.89	1.28	-0.02	0.25	0.16
2.4	1.608	0.70	1.19	-0.04	0.235	0.145
2.5	1.681	0.52	1.10	-0.06	0.21	0.13

For each mass the bolometric magnitude, M_b, was calculated. To fit the main sequence the effective temperature was shifted. M_v and (B-V) are the starting positions (on the main sequence) and t_1 and t_2 are the hydrogen burning times.

TABLE V

Age Estimates for the Evolved Stars

Gliese No.	M_V	B-V	Q	Age Estimate (10^9 years)
8.00	1.37	0.34	3	1.40 ± 0.15
10.00	3.80	0.49	3	2.8 ± 1.5
19.00	3.80	0.62	2	12.0 ± 2.0
34.10	3.40	0.50	5	4.5 ± 0.5
54.21	3.50	0.46	3	3.0 ± 0.5
55.31	3.30	0.47	4	3.5 ± 0.5
58.10	1.20	0.13	6	0.8 ± 0.2
61.00	3.06	0.54	3	7.0 ± 1.0
78.10	1.90	0.48	4	1.9 ± 0.5
80.00	1.70	0.13	4	0.7 ± 0.1
83.00	2.10	0.28	6	1.0 ± 0.4
105.60	3.30	0.59	5	8.0 ± 2.5
124.00	3.72	0.60	3	10.0 ± 1.0
127.00	3.30	0.51	3	5.7 ± 0.5
143.21	3.40	0.39	3	0.7 ± 0.5
147.00	3.21	0.57	3	7.0 ± 1.5
155.00	3.10	0.42	3	2.5 ± 0.5
177.10	4.20	0.65	4	12.0 ± 2.0
197.0	3.84	0.62	3	10.0 ± 2.0
240.10	3.80	0.50	3	3.5 ± 1.0
242.00	2.10	0.43	3	2.0 ± 0.5
264.11	4.30	0.65	3	12.0 ± 2.0
279.00	3.30	0.51	4	5.5 ± 1.0
280.01	2.64	0.42	1	2.8 ± 0.1
284.00	3.80	0.77	4	10.0 ± 2.0
297.10	3.50	0.43	3	1.5 ± 1.0
299.21	3.80	0.49	4	3.5 ± 1.0
305.00	2.50	0.40	5	2.3 ± 0.4
335.01	3.40	0.49	4	4.0 ± 1.0
354.01	2.00	0.46	4	2.0 ± 0.6
397.20	3.50	0.50	4	5.0 ± 1.0
449.00	3.60	0.55	2	7.5 ± 0.5
527.01	3.50	0.48	3	3.5 ± 0.7
549.01	3.22	0.50	3	5.0 ± 0.6
550.21	3.10	0.74	4	6 ± 2
580.20	3.60	0.53	3	6.0 ± 0.7
609.10	2.30	0.52	4	3.0 ± 0.1
657.00	2.10	0.40	4	1.9 ± 0.4
681.00	0.96	0.15	2	0.9 ± 0.05
721.00	0.50	0.0	2	0.4 ± 0.05
725.20	2.80	0.46	3	3.5 ± 0.5
743.11	3.70	0.52	3	5 ± 1
759.00	4.00	0.78	4	12 ± 2
767.11	3.35	0.46	3	3.4 ± 0.7
794.00	3.70	0.53	4	6 ± 1

Table V (continued)

Gliese No.	M_V	B-V	Q	Age Estimate (10^9 years)
805.00	3.70	0.43	3	1.2 ± 1.0
822.11	2.32	0.40	3	2.2 ± 0.3
826.00	1.50	0.22	3	1.15 ± 0.05
836.61	3.10	0.49	3	4.5 ± 0.5
837.00	2.00	0.29	5	1.4 ± 0.1
848.00	3.14	0.44	2	3.4 ± 0.3
855.11	4.30	0.65	4	12 ± 2
872.01	2.60	0.50	4	3.6 ± 1.0
881.00	2.03	0.09	2	0.3 ± 0.2
904.00	3.39	0.51	2	5.5 ± 0.5
512.10	3.60	0.71	4	9 ± 2
602.00	3.35	0.57	3	7.0 ± 1.4
770.10	3.60	0.75	5	9 ± 2
771.01	3.00	0.86	3	5 ± 2
600.00	3.60	0.79	4	8 ± 2
635.01	2.97	0.64	1	6.0 ± 0.5
695.01	3.89	0.75	2	11 ± 1

TABLE VI

Age Estimates for the Upper Main Sequence Stars

Gliese No.	M_V	B-V	Q	Age Estimate (10^9 years)
6.00	4.20	0.47	4	1.5 ± 1.0
20.00	2.80	0.17	4	0.5 ± 0.3
31.11	2.60	-0.01	5	0.3 ± 0.3
106.11	1.90	0.09	3	0.3 ± 0.2
107.01	3.62	0.49	2	2.0 ± 0.4
111.00	3.70	0.48	4	2.5 ± 1.5
121.00	2.40	0.16	4	0.5 ± 0.3
167.10	3.10	0.31	5	0.5 ± 0.3
174.11	2.90	0.34	4	0.8 ± 0.6
176.10	3.50	0.38	4	0.8 ± 0.6
178.00	3.76	0.46	2	1.4 ± 0.4
187.00	3.80	0.42	4	0.7 ± 0.6
189.20	3.50	0.45	4	2.0 ± 0.6
196.00	3.70	0.48	3	2.5 ± 1.5
209.10	3.60	0.46	4	1.6 ± 0.6
217.10	1.80	0.10	3	0.3 ± 0.2
219.00	2.50	0.17	3	0.4 ± 0.3
225.00	2.80	0.33	4	0.9 ± 0.5
244.01	1.42	0.00	1	0.1 ± 0.05
248.00	2.10	0.21	4	0.6 ± 0.3
249.10	3.50	0.45	4	2.0 ± 0.6
268.10	2.80	0.32	4	0.8 ± 0.6
271.01	2.46	0.34	3	1.4 ± 0.3
274.01	2.84	0.32	3	0.8 ± 0.6
278.01	1.14	0.04	2	0.4 ± 0.1
303.00	4.10	0.47	3	1.2 ± 1.0
306.00	4.30	0.46	3	1.2 ± 1.0
321.31	0.50	0.04	4	0.5 ± 0.05
331.01	2.24	0.19	3	0.5 ± 0.4
332.01	3.50	0.37	2	1.1 ± 0.8
333.10	3.60	0.42	3	1.2 ± 0.8
333.30	2.50	0.14	5	0.3 ± 0.2
339.20	0.30	0.01	4	0.5 ± 0.1
348.01	3.90	0.45	3	1.4 ± 1.0
351.01	3.18	0.36	3	0.8 ± 0.5
391.00	3.30	0.36	4	0.8 ± 0.6
403.10	3.70	0.46	3	2.0 ± 1.5
419.00	1.40	0.12	5	0.7 ± 0.3
448.00	1.54	0.08	3	0.5 ± 0.3
455.30	3.10	0.32	3	0.5 ± 0.4
459.00	1.90	0.08	3	0.3 ± 0.2
471.20	2.90	0.37	5	1.1 ± 1.0
482.01	3.46	0.36	3	0.6 ± 0.5
501.01	3.69	0.45	3	1.4 ± 0.8

Table VI (continued)

Gliese No.	M_V	B-V	Q	Age Estimate (10^9 years)
503.00	3.70	0.48	3	2.5 ± 1.5
508.10	1.30	0.03	3	0.3 ± 0.1
525.10	2.70	0.38	4	1.3 ± 0.3
557.00	3.20	0.37	4	0.6 ± 0.5
560.01	2.00	0.24	3	0.8 ± 0.3
563.40	3.90	0.41	4	0.8 ± 0.6
564.10	1.50	0.15	4	0.7 ± 0.2
578.00	3.70	0.43	3	1.0 ± 0.8
594.00	3.40	0.41	3	1.5 ± 1.0
601.00	2.40	0.29	4	0.8 ± 0.6
603.00	3.40	0.48	3	4.6 ± 1.0
615.21	4.00	0.50	3	2.0 ± 1.5
648.00	3.70	0.48	3	2.5 ± 1.5
656.11	1.40	0.06	3	0.4 ± 0.2
670.01	3.30	0.40	3	1.4 ± 1.2
673.10	2.60	0.28	4	0.5 ± 0.4
686.20	3.10	0.40	4	1.2 ± 1.0
692.00	3.60	0.47	4	2.5 ± 2.0
694.11	3.00	0.43	3	2 ± 1
700.11	3.50	0.39	5	1.0 ± 0.8
708.10	3.40	0.40	3	1.2 ± 1
713.00	4.13	0.49	2	2 ± 1
760.00	2.60	0.32	3	0.8 ± 0.2
764.20	3.70	0.50	5	2.5 ± 2
765.01	3.20	0.39	4	1.0 ± 0.8
768.00	2.24	0.22	1	0.6 ± 0.1
773.40	3.90	0.49	3	2.0 ± 1.5
822.01	3.93	0.50	3	2.0 ± 1.5
849.10	3.60	0.49	4	3.1 ± 1.5
886.20	3.60	0.29	5	0.6 ± 0.5
891.10	2.80	0.30	3	0.5 ± 0.4
482.02	3.48	0.29	2	0.6 ± 0.5

TABLE VII

Quality Classes

Quality (Q)	Uncertainty range
1	<0.08
2	0.09--0.15
3	0.16--0.25
4	0.26--0.35
5	0.36--0.50
6	>0.50

TABLE VIII

Cluster Ages

Cluster	Age (10^9 years)			
	Fig. 3	Lindoff (1968)	Sandage and Eggen	Iben (1967)
NGC 188	10.0	6.4	9 ± 1	11 ± 2
M 67	6.0	4.0	5.5	5.5 ± 1
NGC 3680	3.2			
NGC 7789	2.0	0.9		
Hyades	1.4	0.7		
M 11	0.3			

TABLE IX

Age Estimates for the Giants

Gliese No.	M_V	B-V	Q	Age Estimate (10^9 years)
31.00	0.70	1.01	3	2.0 ± 0.7
81.01	2.70	0.85	4	4.5 ± 1.0
84.30	0.60	1.15	3	1.4 ± 0.5
150.00	3.77	0.92	1	10 ± 1
154.20	2.30	1.13	5	10 ± 2
167.30	3.50	1.06	4	10 ± 1
171.11	-0.60	1.54	3	?
194.01	0.09	0.80	2	0.7 ± 0.2
224.01	3.00	1.05	6	7 ± 2
286.00	0.98	1.00	2	1.5 ± 0.4
321.10	2.50	0.87	5	4 ± 1
412.10	3.30	1.03	5	8 ± 2
534.00	2.72	0.58	2	5.0 ± 0.5
539.00	1.20	1.00	4	2.0 ± 0.5
541.00	-0.24	1.23	2	?
624.11	1.00	0.91	5	1.6 ± 0.4
626.10	2.70	0.91	4	4.5 ± 1.0
636.00	1.80	0.92	4	3.0 ± 0.5
639.10	1.10	1.16	5	?
711.00	1.80	0.94	4	3.0 ± 0.5
806.11	0.80	1.03	4	2.0 ± 0.5
807.00	2.72	0.92	2	5.5 ± 0.5
893.21	1.80	1.11	5	7 ± 2
903.00	2.27	1.03	3	6 ± 1
835.10	2.30	0.99	5	4.5 ± 2.0
239.10	2.60	1.05	3	7 ± 1
596.20	1.10	1.17	3	4 ± 2
355.10	2.90	0.77	4	4.5 ± 1.5
894.21	3.60	0.79	4	8 ± 2
355.20	3.20	1.02	4	9 ± 2
532.10	4.60	1.02	6	10 ± 2

TABLE X

Uncertainties in the Ages and Velocity Dispersions

Group	Number	Mean Age (10^9 years)	Age Uncertainty	Velocity Dispersion (km/sec)	Lower Limit (70% confidence)	Upper Limit
1	22	0.38	0.07	15.5	13.5	18.7
2	21	0.72	0.12	16.8	14.6	20.5
3	21	1.16	0.18	18.3	16.0	22.2
4	20	1.72	0.18	21.6	18.8	26.3
5	16	2.32	0.38	28.4	24.2	35.7
6	15	3.23	0.21	30.8	26.2	39.1
7	19	4.67	0.26	30.3	26.0	37.3
8	16	6.81	0.37	35.3	30.1	44.4
9	16	10.50	0.45	46.1	39.2	58.0
white dwarfs	22			49.9	43.4	60.3
sub-dwarfs	18			56.0	48.1	68.8

TABLE XI

Velocity Distributions of the Various Age Groups

Group	Mean Velocities (km/sec) u	v	w	Velocity Dispersions (km/sec) σ_u	σ_v	σ_w	Vertex Deviation (°)
1	- 3.0	- 5.0	- 6.8	15.5	9.0	5.4	13.9
2	-12.8	- 6.6	- 8.2	16.8	10.9	7.1	26.4
3	-11.9	-11.9	- 8.4	18.3	10.8	12.6	20.0
4	-14.8	-10.5	-10.3	21.6	15.3	10.2	12.4
5	- 9.7	-12.1	- 5.6	28.4	19.8	15.9	2.1
6	-11.6	-11.6	-13.7	30.8	21.3	12.2	-14.6
7	- 8.7	-20.1	- 4.8	30.3	22.9	16.3	22.5
8	- 8.4	-21.1	-14.6	35.3	20.5	21.2	3.2
9	-34.2	-35.1	-11.7	46.1	30.4	19.9	20.1

TABLE XIII

Parameters of the Spiral Pattern

Parameter	Numerical Value
A (Strength of spiral field)	5% of the mean galactic gravitational field
i (Angle of inclination of arms)	$6^{\circ}.2$
w (Pattern angular velocity)	13.5 km/sec/kpc
r_o (Reference position)	(8.26 kpc, 0°)
n (Number of arms)	2

TABLE XIV

Comparison of Results for the Time-independent Case

Velocity Dispersion (km/sec)	Mean Radial Velocity (km/sec)		Mean Transverse Velocity (km/sec)	
	Our results	Lin	Our Results	Lin
15	8.52	8.56	3.03	3.01
20	5.68	5.72	0.88	0.895
24	4.13	4.16	0.22	0.23

TABLE XV

Variation of the Mean Radial Velocity

Radial Velocity Dispersion (km/sec)	Axis Ratio 0.20	0.30	0.40	0.50	0.60	
18	7.02	8.49	9.63	10.53	11.25	$\ell=0^\circ$
20	5.41	6.38	7.08	7.61	7.96	
22	4.34	4.98	5.42	5.74	5.89	
24	3.57	4.00	4.29	4.48	4.55	
28	2.54	2.74	2.98	2.91	2.98	
18	13.51	11.50	11.12	11.22	11.46	$\ell=10^\circ$
20	9.10	8.07	7.76	7.83	7.90	
22	6.67	6.00	5.67	5.76	5.73	
24	5.18	4.66	4.35	4.43	4.39	
28	3.44	3.04	2.93	2.82	2.86	

TABLE XVI

Variation of the Mean Tangential Velocity

Radial Velocity Dispersion (km/sec)	Axis Ratio 0.20	0.30	0.40	0.50	0.60	
18	-2.27	-2.10	-1.90	-1.75	-1.60	$\ell=0^\circ$
20	-1.08	-1.00	-0.88	-0.78	-0.69	
22	-0.32	-0.34	-0.30	-0.25	-0.21	
24	0.16	0.05	0.03	0.04	0.04	
28	0.59	0.41	0.35	0.26	0.28	
18	-5.84	-3.84	-2.92	-2.41	-2.07	$\ell=10^\circ$
20	-3.05	-2.04	-1.49	-1.18	-0.98	
22	-1.50	-0.98	-0.66	-0.49	-0.39	
24	-0.57	-0.33	-0.16	-0.10	-0.08	
28	0.38	0.34	0.31	0.27	0.26	

TABLE XVII

Variation of the Radial Velocity Dispersion

Radial Velocity Dispersion (km/sec)	Axis Ratio 0.20	0.30	0.40	0.50	0.60	
18	17.30	15.45	13.57	11.61	9.36	$\ell=0°$
20	20.17	19.05	17.98	17.00	16.00	
22	22.54	21.78	21.04	20.39	19.73	
24	24.71	24.14	23.59	23.09	22.61	
28	28.75	28.36	27.99	27.65	27.42	
18	16.89	15.66	14.12	12.43	10.35	$\ell=10°$
20	21.25	19.92	18.82	17.74	16.66	
22	23.73	22.64	21.80	20.96	20.20	
24	25.75	24.89	24.18	23.51	22.90	
28	29.51	28.86	28.34	27.92	27.37	

TABLE XVIII

Variation of the Axis Ratio

Radial Velocity Dispersion (km/sec)	Axis Ratio 0.20	0.30	0.40	0.50	0.60	
18	-0.12	0.11	0.48	1.11	2.39	$\ell=0°$
20	0.01	0.19	0.42	0.70	1.03	
22	0.07	0.22	0.40	0.60	0.82	
24	0.10	0.24	0.40	0.56	0.74	
28	0.13	0.26	0.39	0.53	0.68	
18	-0.12	0.18	0.52	1.03	2.03	$\ell=10°$
20	0.07	0.23	0.42	0.67	0.98	
22	0.12	0.25	0.40	0.59	0.80	
24	0.13	0.26	0.39	0.56	0.73	
28	0.16	0.27	0.40	0.53	0.67	

TABLE XIX

Variation of the Vertex Deviation

Radial Velocity Dispersion (km/sec)	Axis Ratio 0.20	0.30	0.40	0.50	0.60	
18	-4.73	-10.47	-23.32	-48.64	-66.30	$\ell=0^\circ$
20	-5.10	-9.04	-15.41	-27.06	-46.92	
22	-4.70	-7.45	-11.22	-17.42	-29.39	
24	-4.12	-6.07	-8.45	-12.10	-18.12	
28	-3.05	-4.08	-5.13	-6.49	-9.05	
18	21.86	18.54	19.45	50.86	-82.82	$\ell=10^\circ$
20	11.71	8.79	5.94	1.37	-40.00	
22	8.32	6.29	3.84	2.01	-5.29	
24	7.35	5.91	4.81	3.74	2.35	
28	7.33	6.74	8.71	6.53	7.25	

TABLE XX

Variation of the Density

Radial Velocity Dispersion (km/sec)	Axis Ratio 0.20	0.30	0.40	0.50	0.60	
18	0.53	0.54	0.55	0.55	0.55	$\ell=0^\circ$
20	0.61	0.62	0.62	0.62	0.62	
22	0.67	0.68	0.68	0.68	0.69	
24	0.72	0.73	0.73	0.73	0.74	
28	0.80	0.80	0.80	0.81	0.81	
18	0.46	0.52	0.54	0.55	0.55	$\ell=10^\circ$
20	0.57	0.61	0.62	0.63	0.63	
22	0.66	0.68	0.69	0.69	0.69	
24	0.72	0.74	0.74	0.74	0.74	
28	0.80	0.81	0.81	0.81	0.81	

TABLE XXI

Comparison of Angular Velocities and Epicyclic Frequencies

Galacto-centric Distance R (kpc)	Angular Velocity Ω (km/sec/kpc)		Epicyclic Frequency K (km/sec/kpc)	
	Schmidt	Polynomial (20)	Schmidt	Polynomial (21)
6	39.7	39.6	62.8	63.4
7	35.3	35.4	54.4	54.1
8	31.5	31.5	46.7	45.8
9	28.1	28.1	39.2	38.7
10	25.0	24.9	31.6	32.3
11	22.2	22.2	26.5	27.1
12	19.8	19.8	22.8	22.9
13	17.8	17.8	20.0	19.7
14	16.1	16.1	17.7	17.5

FIGURES

FIGURE 1

Model tracks from Schlesinger's Formulas

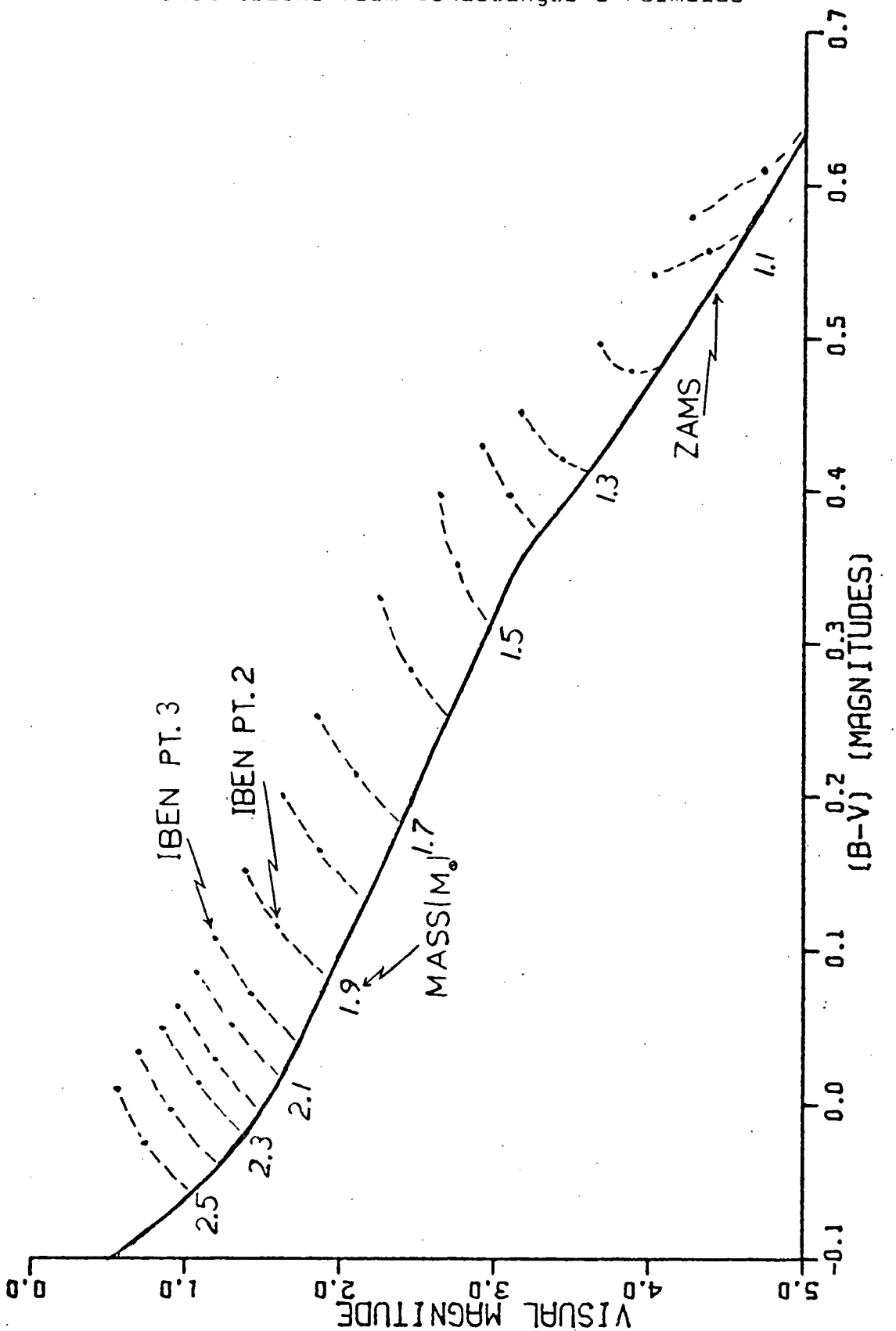

FIGURE 2

Isochrones

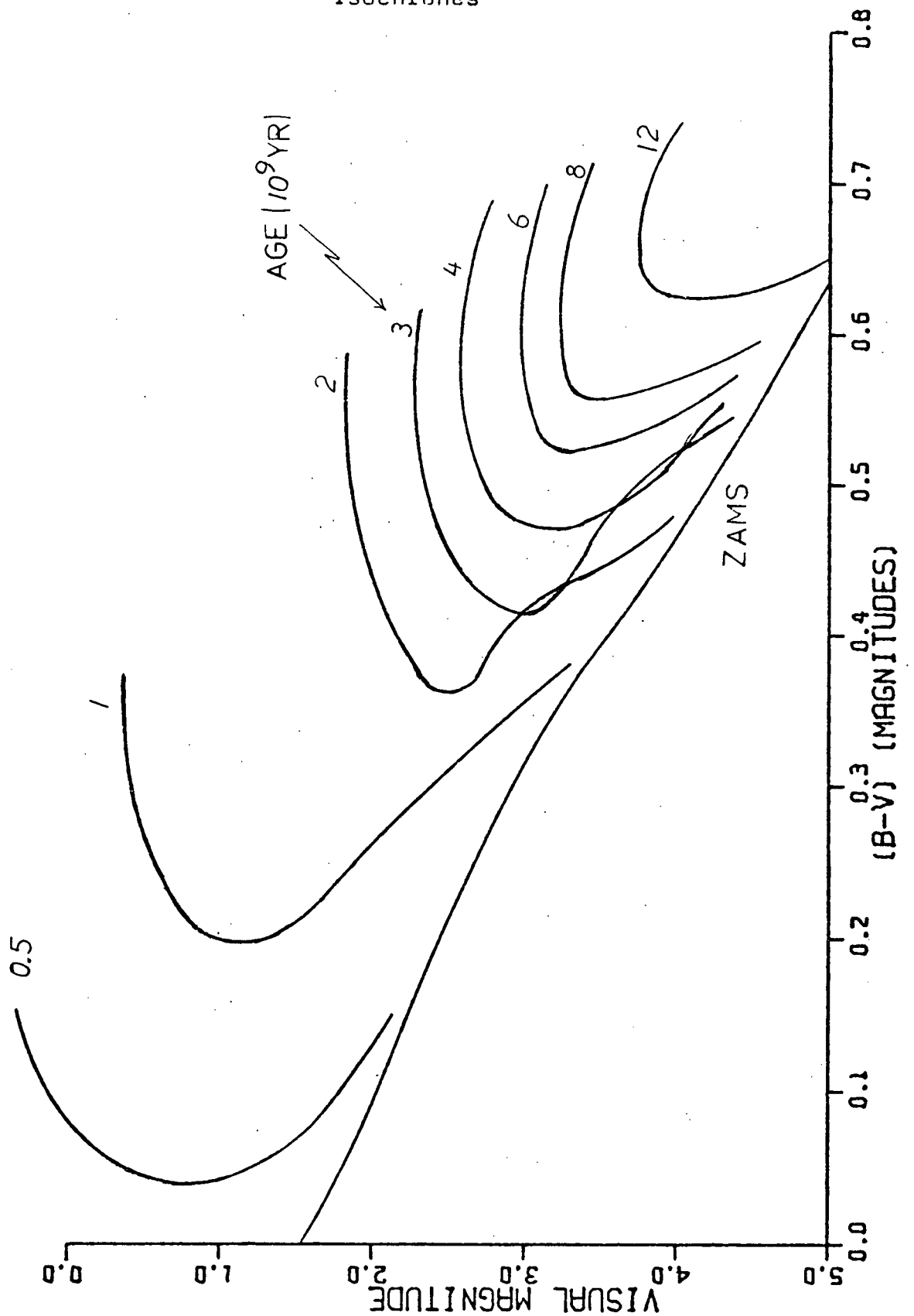

FIGURE 3

Cluster Composite

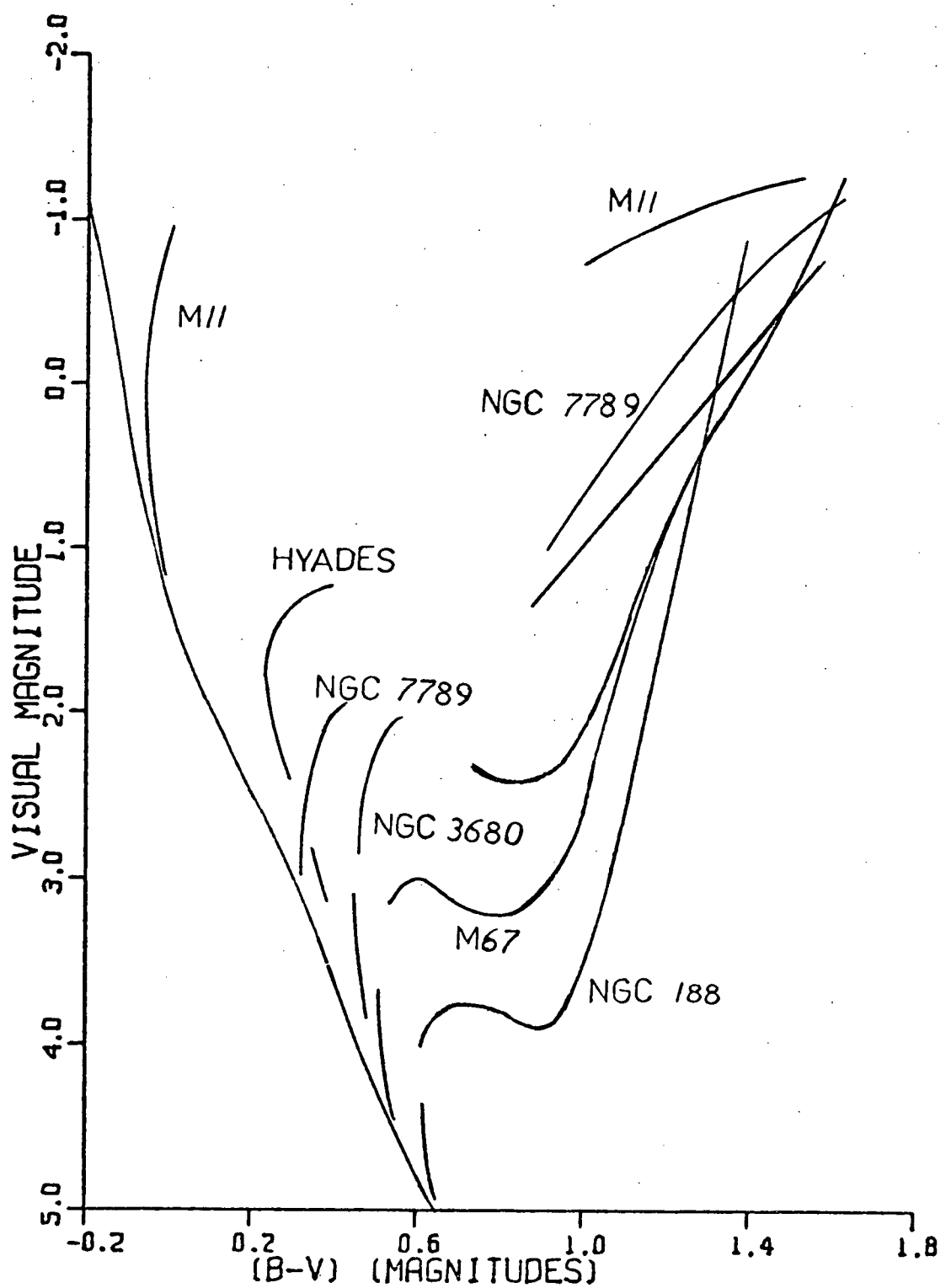

FIGURE 4

Age-dependence of the Velocity Dispersions

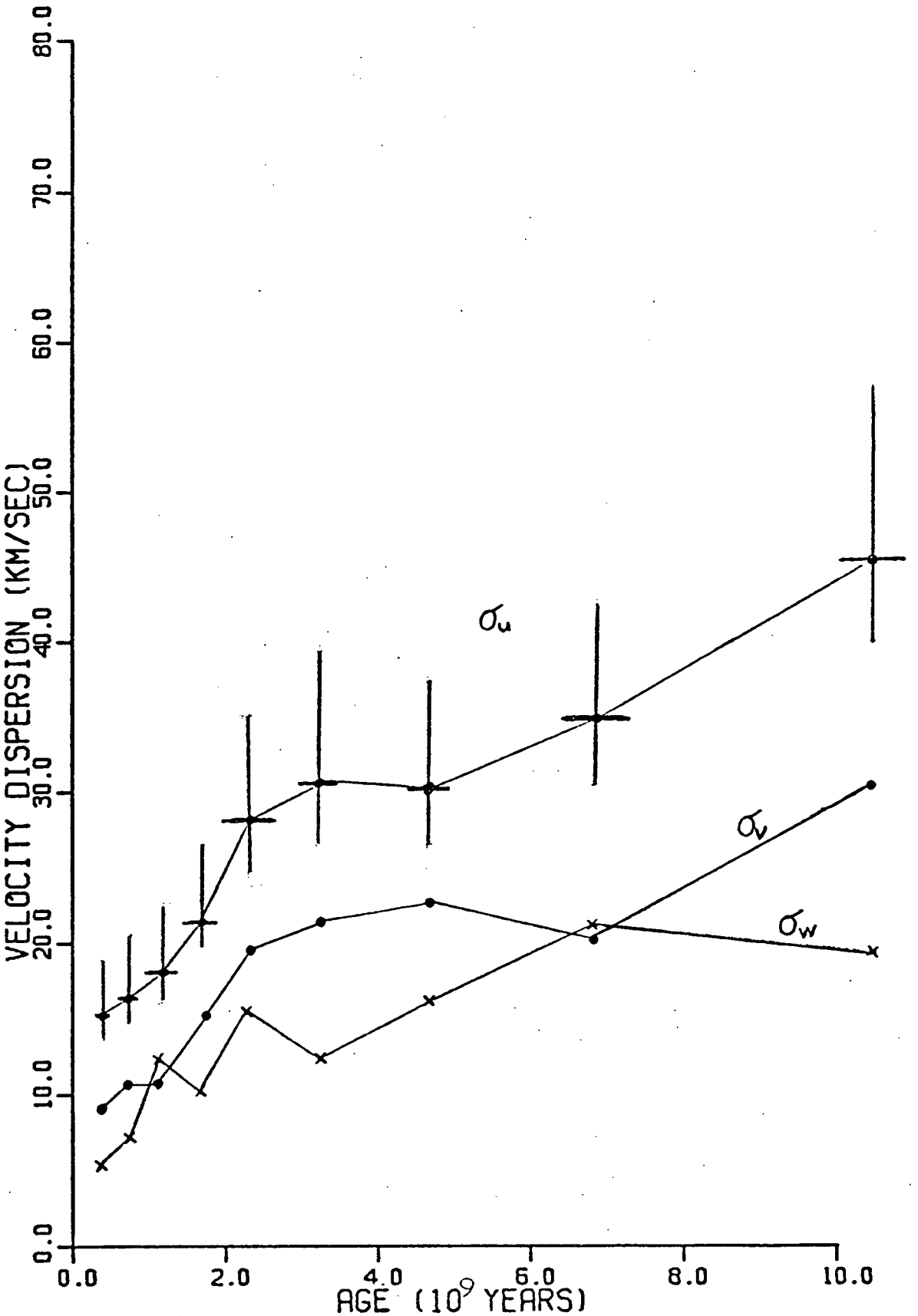

FIGURE 5

Time-dependence of Radial Velocity

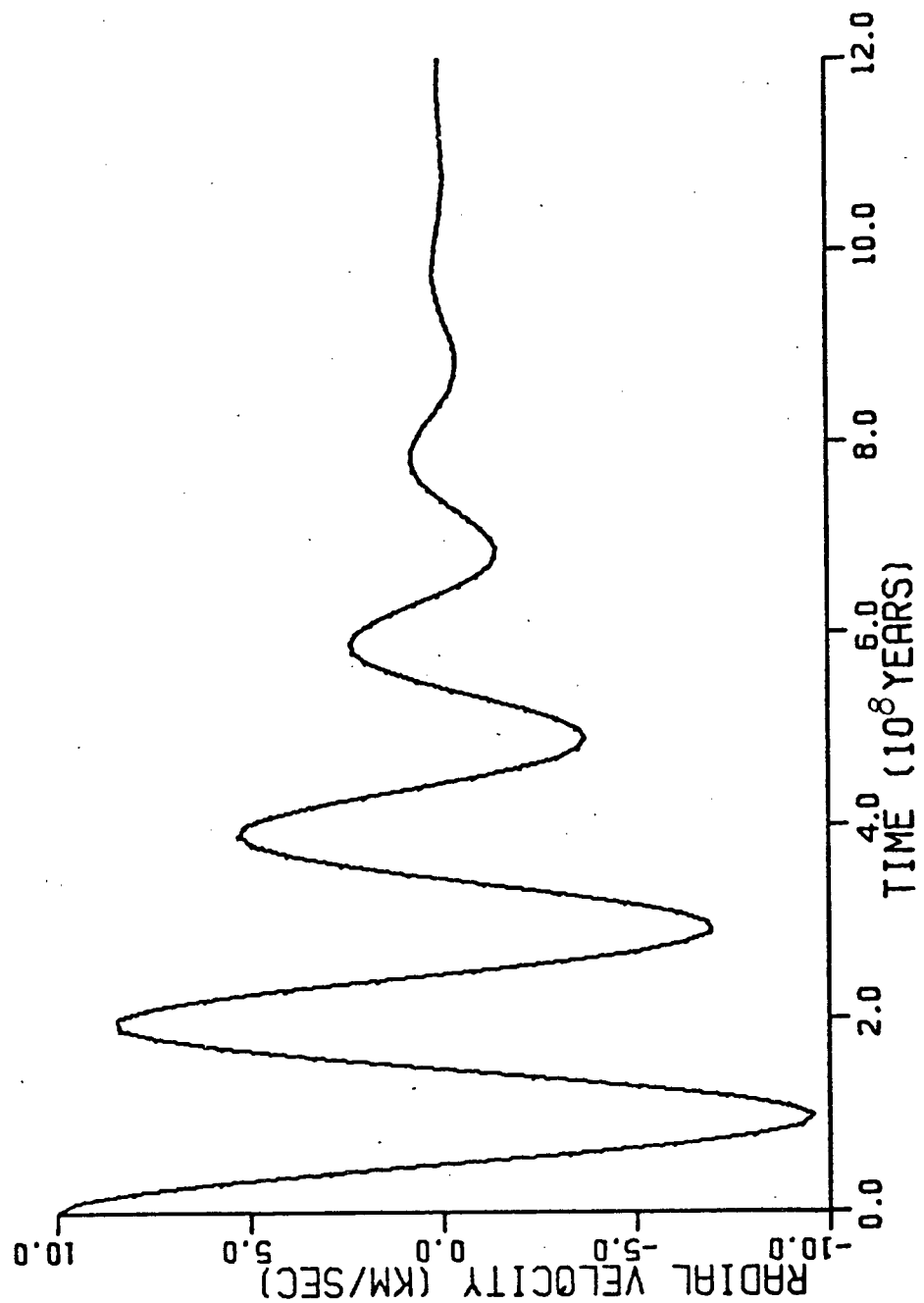

FIGURE 6

Time-dependence of Tangential Velocity

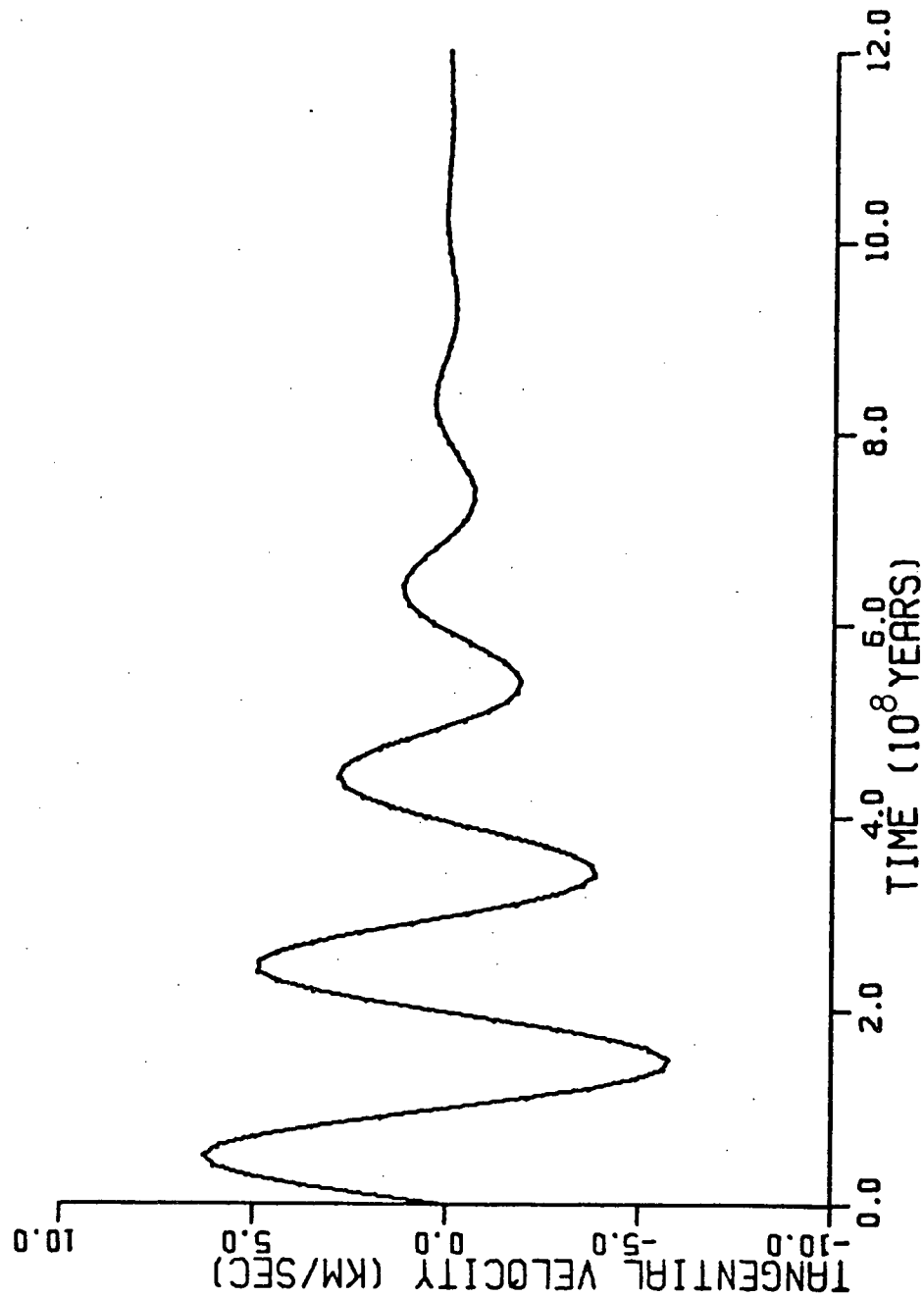

FIGURE 7

Time-dependence of Radial Velocity Dispersion

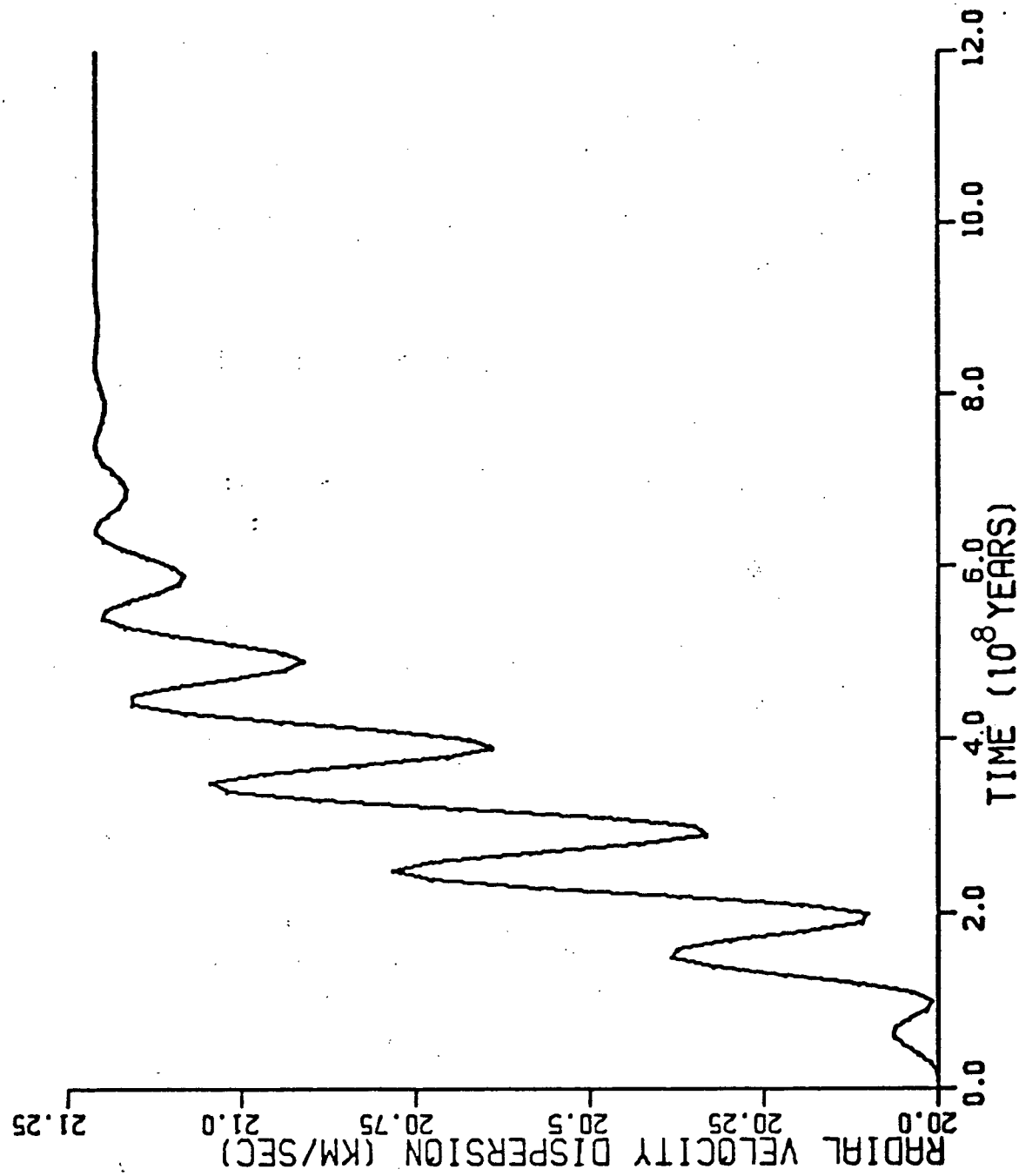

FIGURE 8

Time-dependence of Axis Ratio

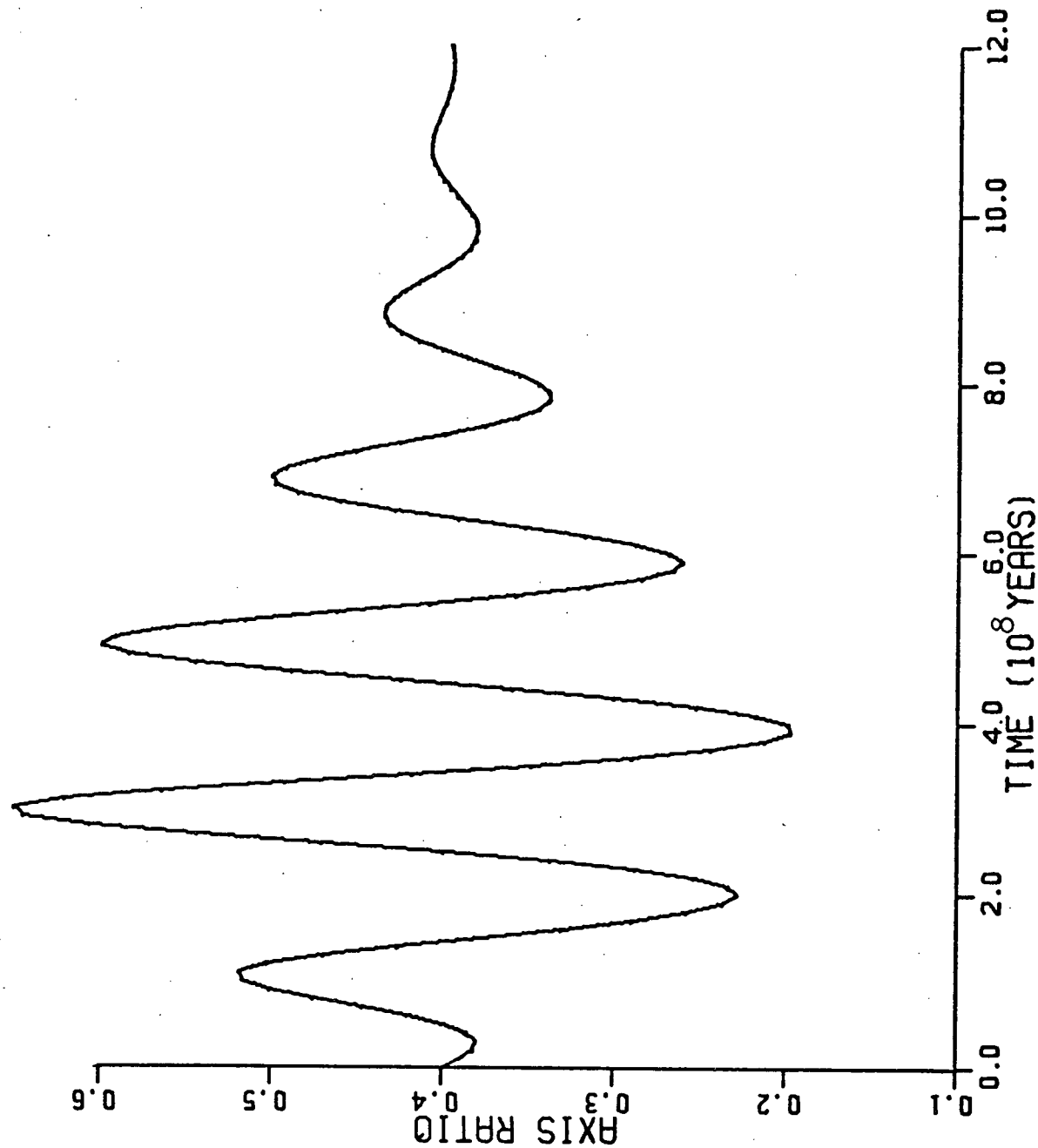

FIGURE 9

Time-dependence of Vertex Deviation

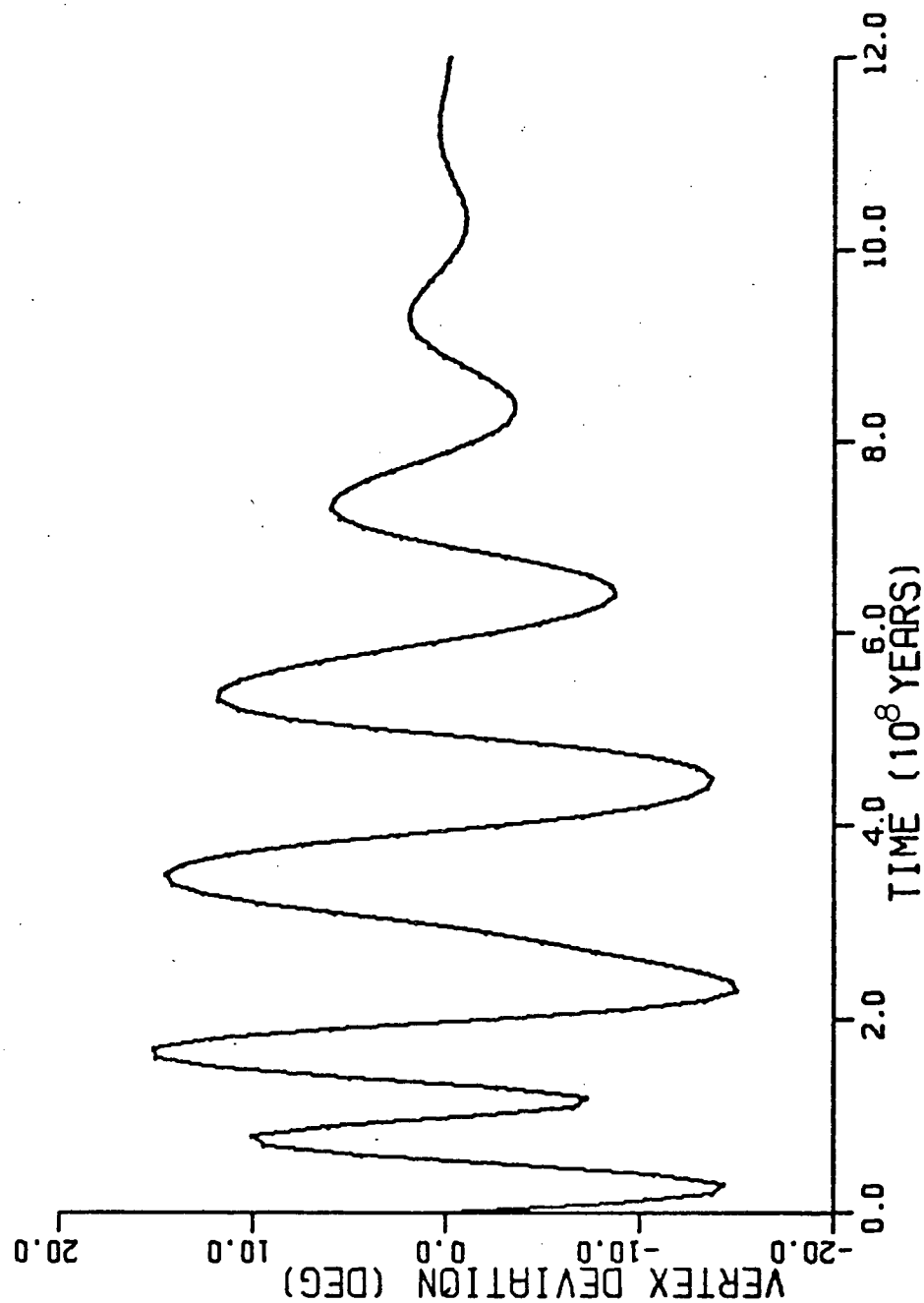

FIGURE 10

Time-dependence of Radial Velocity

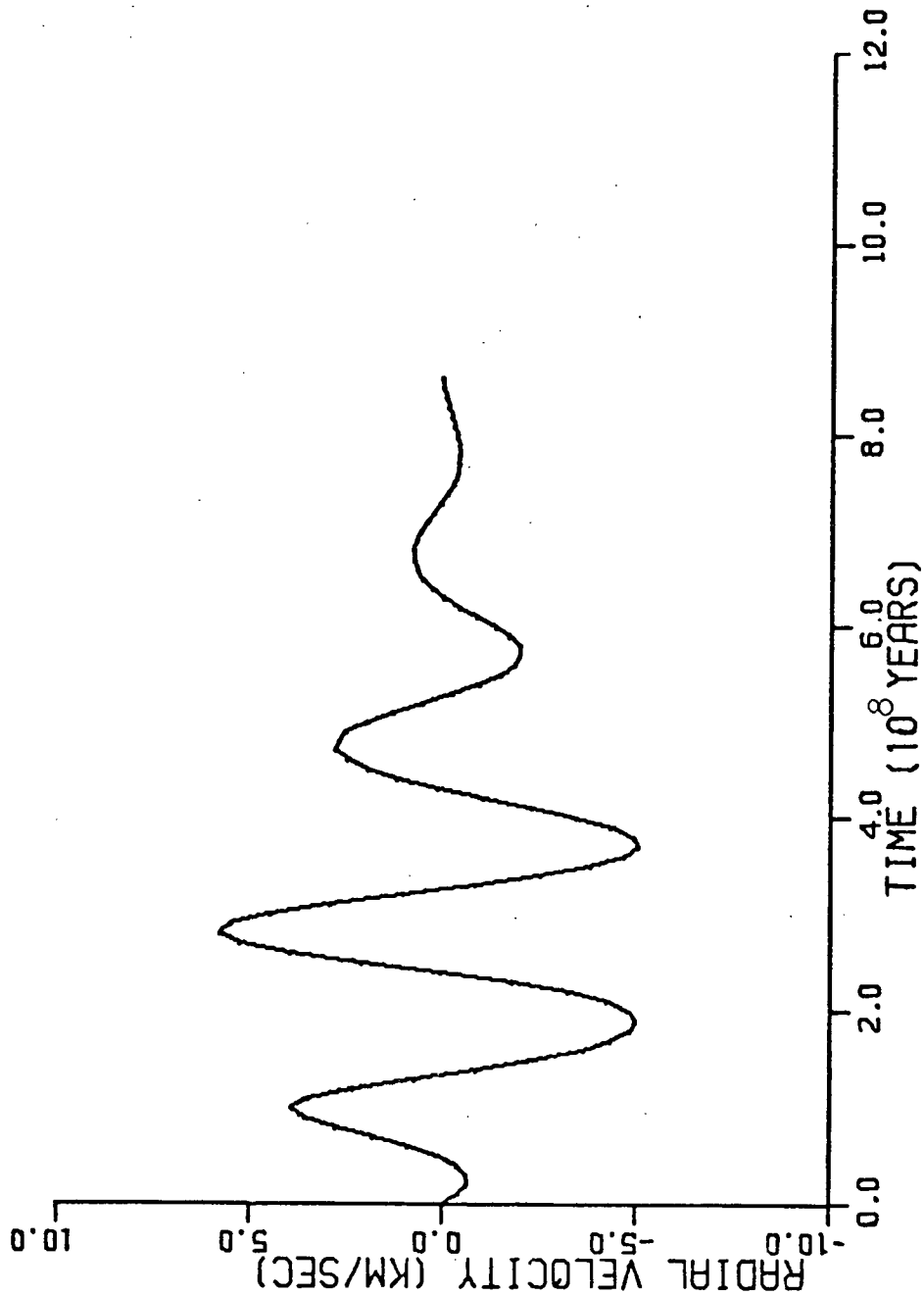

FIGURE 11

Time-dependence of Tangential Velocity

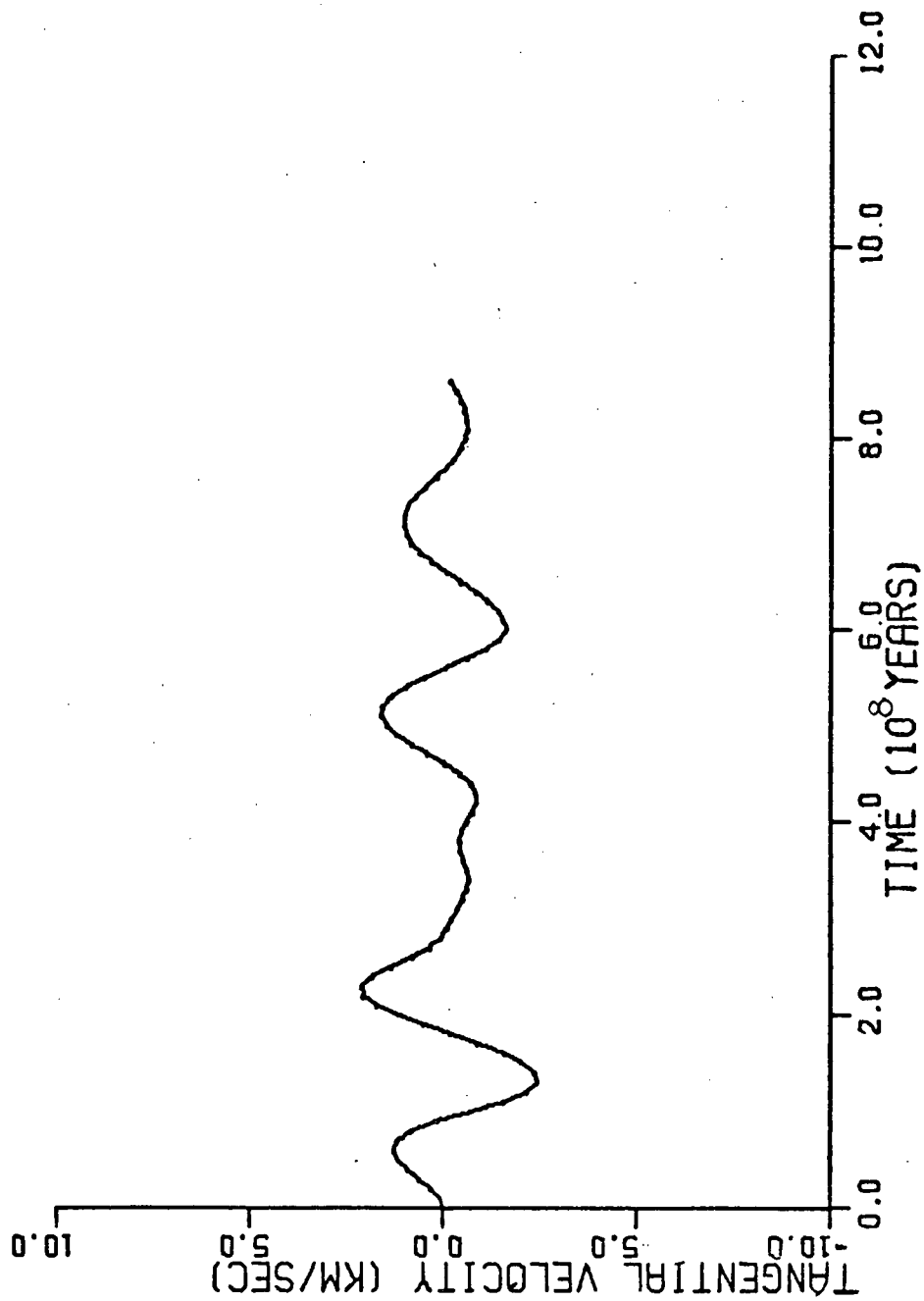

FIGURE 12

Time-dependence of Radial Velocity Dispersion

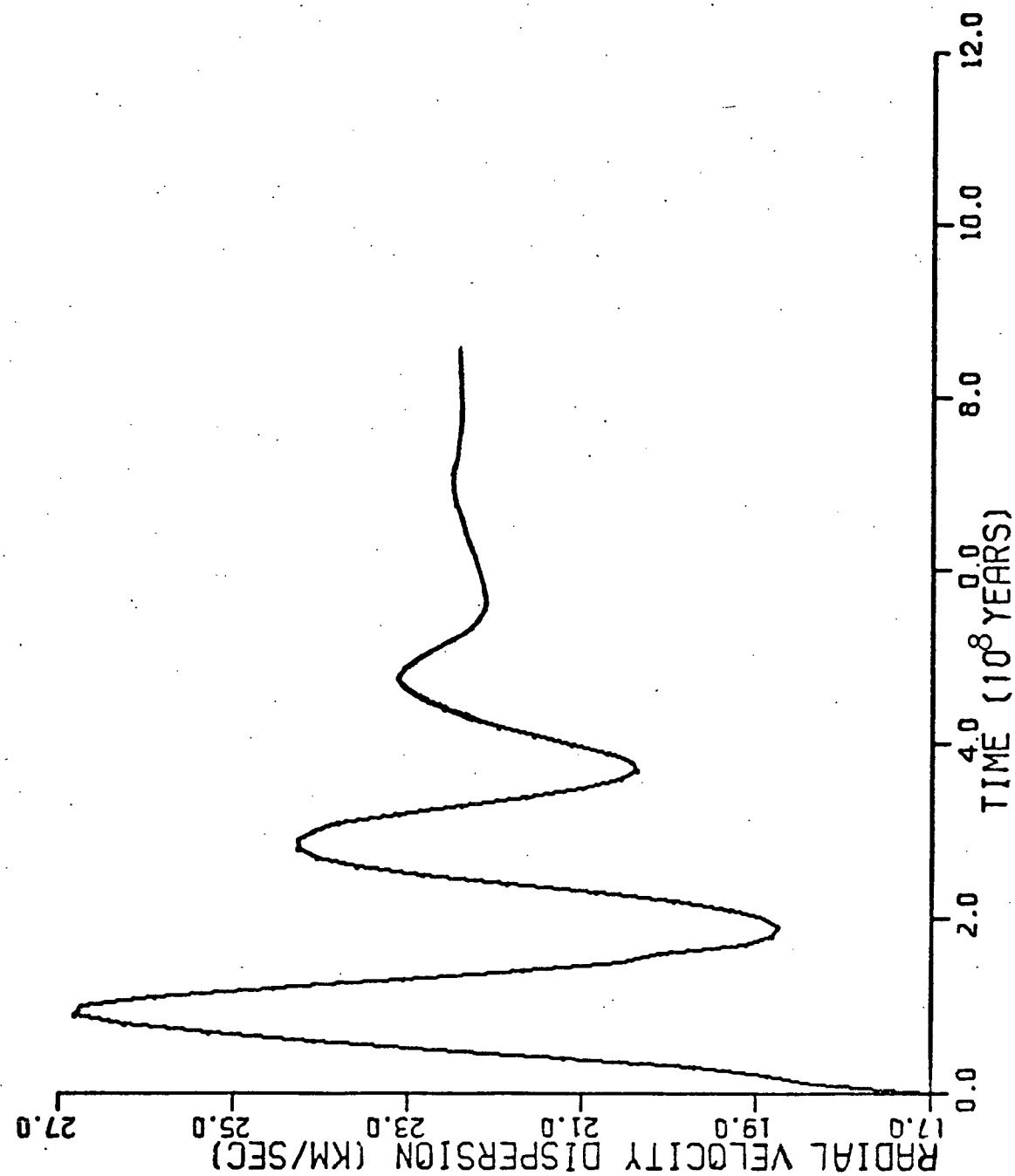

FIGURE 13

Time-dependence of Axis Ratio

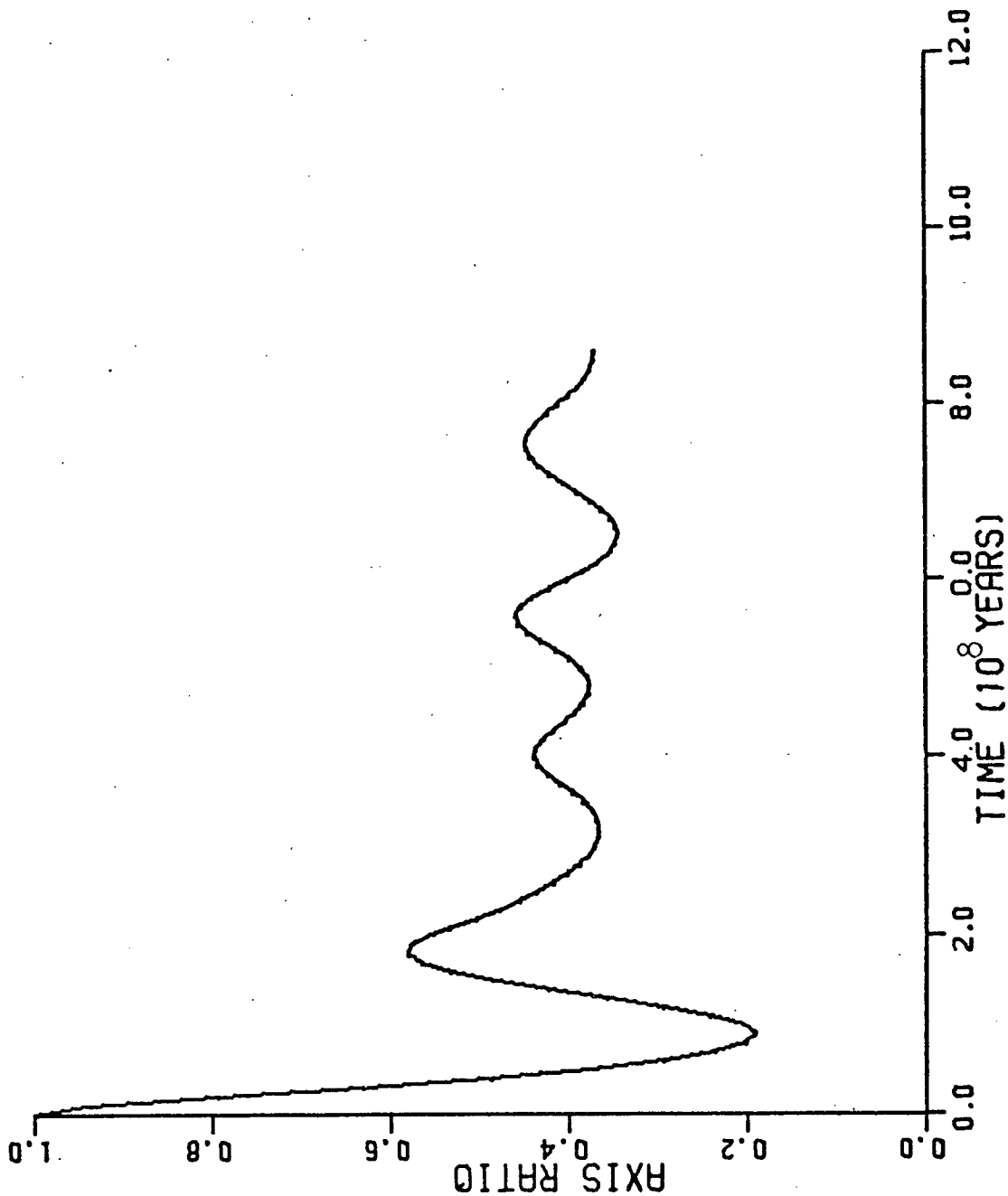

FIGURE 14

Time-dependence of Vertex Deviation

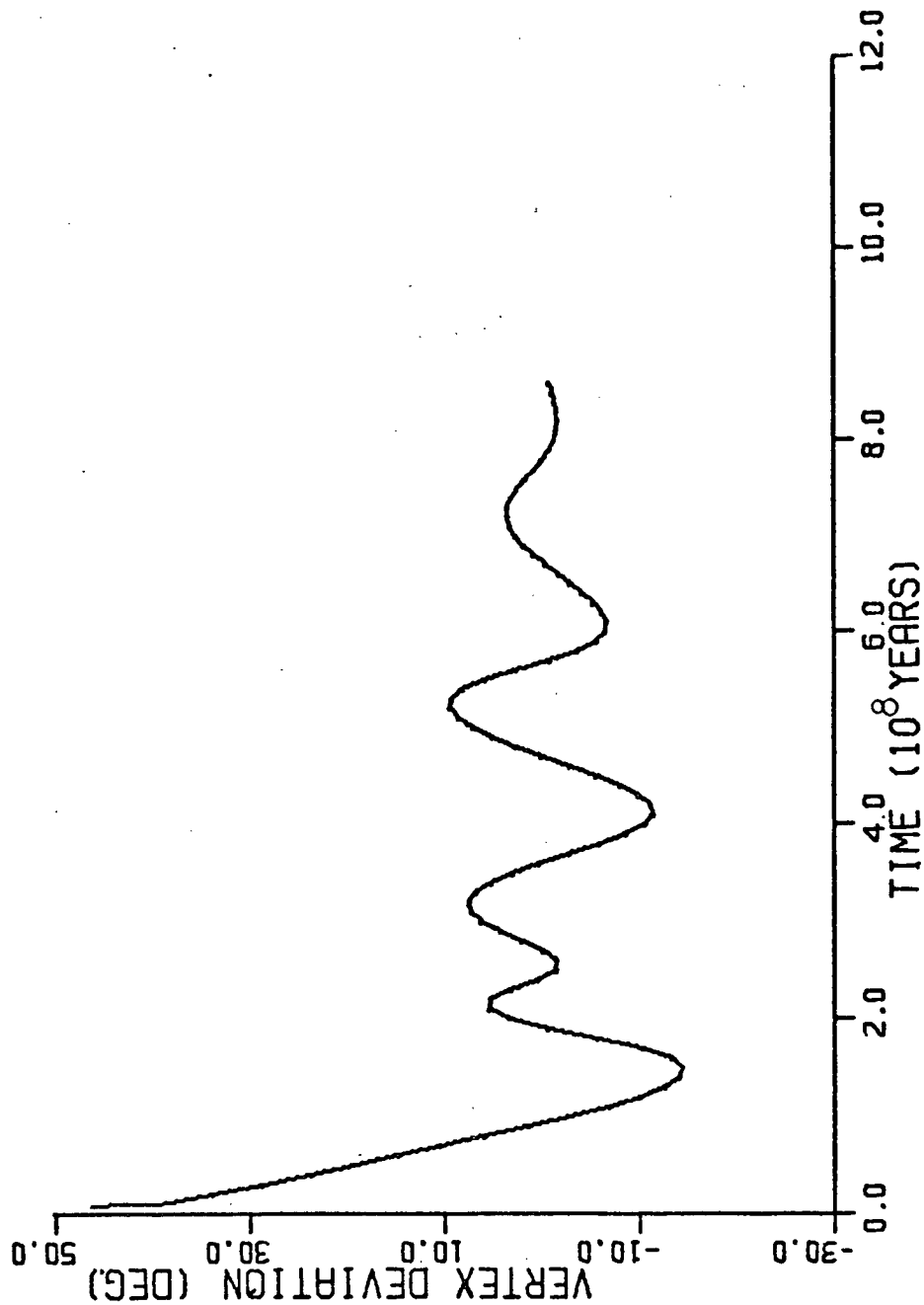

FIGURE 15

Relation between Velocity Dispersion and Vertex Deviation

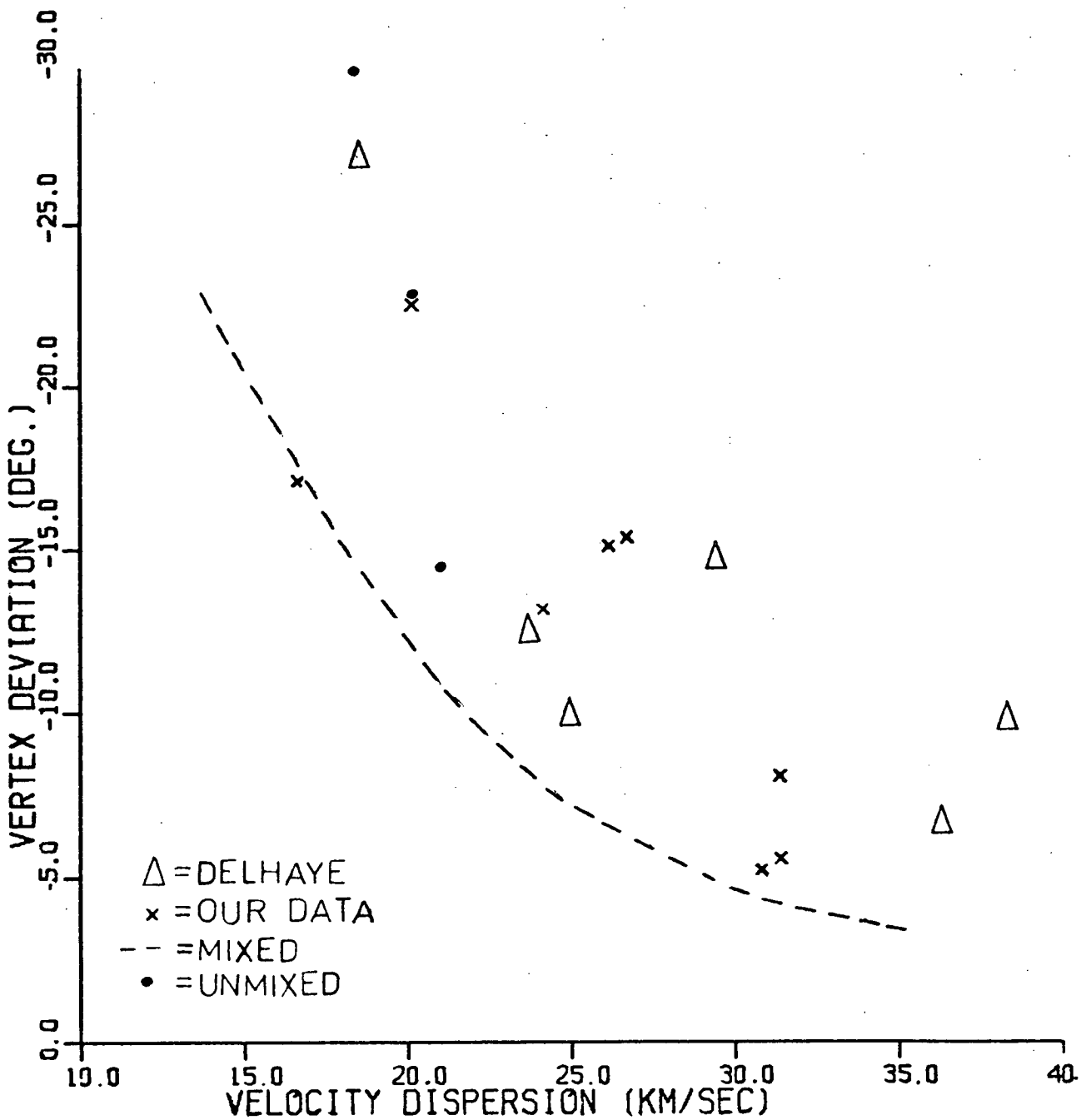

FIGURE 16

Age Dependence of the Radial Velocity Dispersion

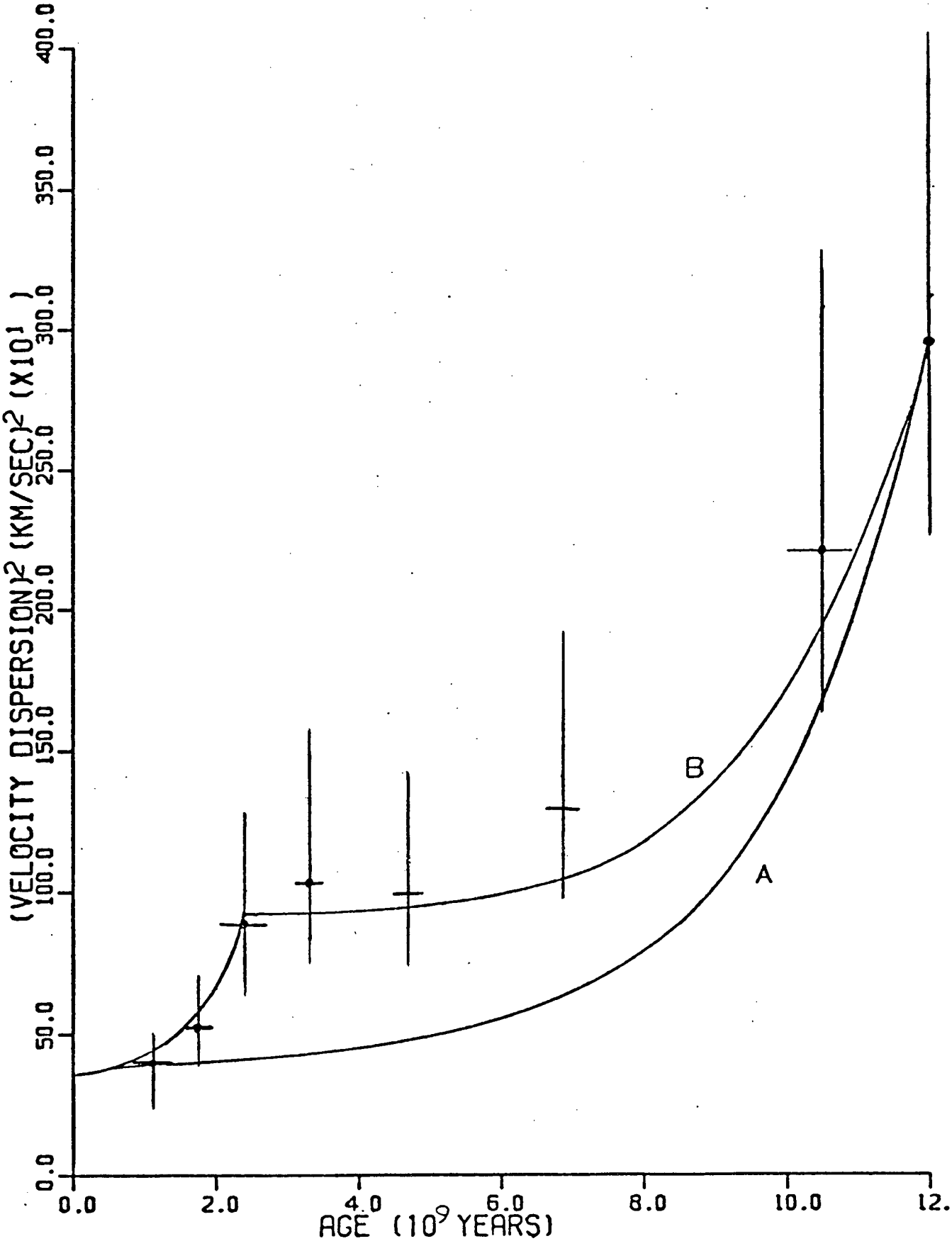

FIGURE 17

Revised Age Dependence of the Radial Velocity Dispersion

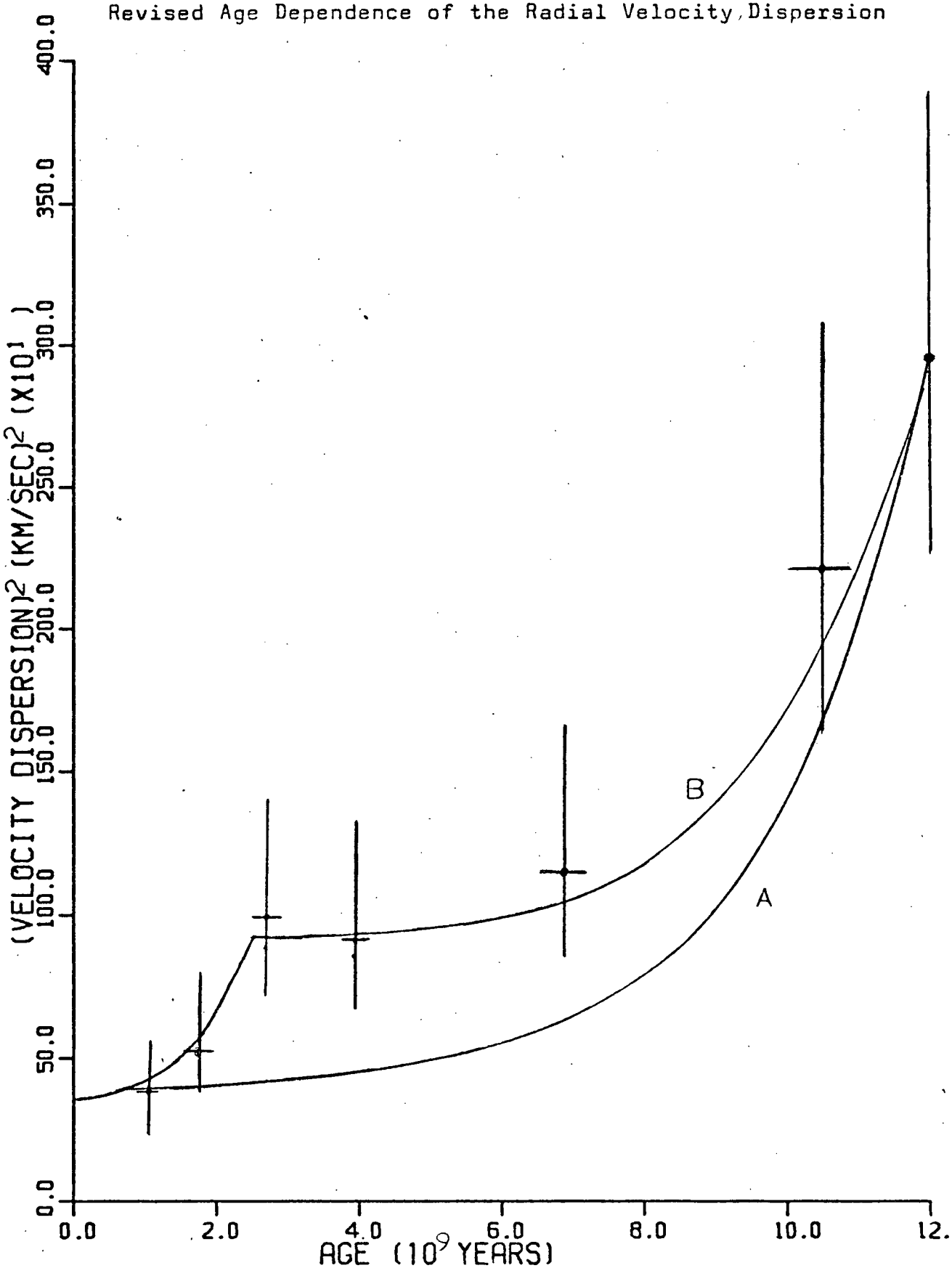

BIBLIOGRAPHY

Allen, C.W. 1963, Astrophysical Quantities, London, Athlone Press.

Barbanis, B., Woltjer, L. 1967, Ap.J. 150, 461

Bernstein, I.B., Trehan, S.K. 1961, Nuclear Fusion 1, 3.

Chandrasekhar, S. 1942, Principles of Stellar Dynamics, Chicago, Univ. of Chicago Press.

Chapman, S., Cowling, T.G. 1953, Mathematical Theory of Non-Uniform Gases, Cambridge, Cambridge University Press.

Chew, G., Goldberger, M., Low, F. 1956, Proc. Roy. Soc. A236, 112.

Delhaye, J. 1965, Stars and Stellar Systems 5, 61.

Demarque, P. 1968, A.J. 73, 669.

Eggen, O.J., Lynden-Bell, D., Sandage, A.R. 1962, Ap.J. 136, 748.

Gliese, W. 1956, Zs.f.Ap. 39, 1

Gliese, W. 1968, Low-Luminosity Stars, Ed. S.S. Kumar, Gordon and Breach, New York, 41.

Gliese, W. 1969, Ver. Ast. Rech.-Inst. Heidelberg No. 22.

Harris, D.L. III 1963, Stars and Stellar Systems 3, 263.

Harrison, E.R. 1970, M.N.R.A.S. 150, 443.

Hunter, C. 1969, Studies in Ap. Math, 49, 59.

Iben, I. 1966, Ap.J. 143, 483, 505, 516.

Iben, I. 1967, Ap.J. 147, 624.

Johnson, H.L. 1963, Stars and Stellar Systems 3, 204.

Johnson, H.L. 1966, A.R.A.A. 4, 193.

Julian, W.H. 1967, Ap.J. 148, 175.

Kalnajs, A.J. 1971, A.J. 76, 665.

Kato, S. 1968, Astrop. & Sp. Sc. 2, 37.

Kitamura, S. 1968, Pub. Ast, Soc, Japan 20, 27.

Lin, C.C., Yuan, C., Shu, F.H. 1969, Ap.J. 155, 723.

Lindoff, U. 1968, Arkiv f. Ast., Bd. 5 Nr. 1.

Marochnik, L.S. 1964, Sov. Ast. 8, 202

Marochnik, L.S., Suchkov, A.A. 1969, Sov. Ast. 13, 252.

Mayor, M. 1970, Astron. & Astrop. 6, 60.

Pomagaev, S.G. 1970, Sov. Ast. 13, 635.

Roberts, W.W. 1970, I.A.U. Syn. No. 38, 415.

Sandage, A.R., Eggen, O.J. 1969, Ap.J. 158, 687

Schlesinger, B. 1969, Ap.J. 157, 532.

Schmidt, M. 1965, Stars and Stellar Systems 5, 513

Schmidt-Kaler, Th. 1965, Numberical Data and Functional Relations I, 297.

Simonson, S.C. 1970, Astron. & Astrop. 9, 1963.

Spitzer, L., Schwarzschild, M. 1953, Ap.J. 118, 106.

Toomre, A. 1964, Ap.J. 139, 1217.

von Hoerner, S. 1960, Fortschritte der Physik 8, 191.

Woolley, R.v.d.R. 1958, M.N.R.A.S. 118, 45.

Woolley, R.v.d.R. 1970, I.A.U. Sym. No. 38, 423.

Watson, G.N. 1922, Theory of Bessel Functions, Cambridge, Cambridge University Press.

Yuan, C. 1969 I, Ap.J. 158, 871.

Yuan, C. 1969 II, Ap.J. 158, 889.

Yuan, C. 1971, A.J. 76, 665.

Lynden-Bell, D. 1962, M.N.R.A.S. 124, 279.

Mihalas, D. 1968, Galactic Astronomy, San Francisco, W. H. Freeman and Co.

Toomre, A. 1969, Ap.J. 158, 899